

State of Oregon
Oregon Department of Geology and Mineral Industries
Ian P. Madin, Interim State Geologist

OPEN-FILE REPORT O-15-02

**LOCAL TSUNAMI EVACUATION ANALYSIS OF SEASIDE AND GEARHART,
CLATSOP COUNTY, OREGON**

by George R. Priest¹, Laura L. Stimely¹, Ian P. Madin², and Rudie J. Watzig²



2015

¹Oregon Department of Geology and Mineral Industries, Coastal Field Office, P.O. Box 1033, Newport, OR 97365

²Oregon Department of Geology and Mineral Industries, 800 NE Oregon Street, Suite 965, Portland, OR 97232

DISCLAIMER

This product is for informational purposes and may not have been prepared for or be suitable for legal, engineering, or surveying purposes. Users of this information should review or consult the primary data and information sources to ascertain the usability of the information. This publication cannot substitute for site-specific investigations by qualified practitioners. Site-specific data may give results that differ from the results shown in the publication.

Oregon Department of Geology and Mineral Industries Open-File Report O-15-02
Published in conformance with ORS 516.030

For additional information:
Administrative Offices
800 NE Oregon Street, Suite 965
Portland, OR 97232
Telephone (971) 673-1555
Fax (971) 673-1562
<http://www.oregongeology.org>
<http://egov.oregon.gov/DOGAMI/>

TABLE OF CONTENTS

1.0 INTRODUCTION	1
2.0 METHODS.....	3
2.1 Tsunami hazard zone layers	4
2.2 Lidar elevations layer.....	4
2.3 Speed Conservation Value (SCV) slope table	7
2.4 Beat-the-Wave (BTW) Modeling	8
3.0 RESULTS	14
4.0 DISCUSSION.....	15
4.1 Key findings	15
4.2 Uncertainties and potential improvements	23
5.0 CONCLUSIONS AND RECOMMENDATIONS	25
6.0 ACKNOWLEDGMENTS	30
7.0 REFERENCES	30

LIST OF FIGURES

Figure 1-1. Portion of DOGAMI (2013) tsunami evacuation map for Seaside-Gearhart.....	2
Figure 2-1. Model diagram of path distance approach from Wood and Schmidtlein (2012)	5
Figure 2-2. Calculation of slope along Broadway Street.....	6
Figure 2-3. Example of the network of least-cost paths from the least-cost-distance (LCD) analysis limited to trails and streets	8
Figure 2-4. Illustration of XXL1 tsunami arrival times after a Cascadia subduction zone earthquake showing locations of three evacuation routes at Seaside	10
Figure 2-5. XXL1 times after the earthquake when simulated tsunami flow depth exceeded 0.5 ft for each evacuation route shown on the map of Figure 2-4	11
Figure 4-1. Evacuation time at 4 fps to reach the eastern bank of the Necanicum River estuary in Seaside with bridges intact	17
Figure 4-2. Evacuation times at 4 fps to reach the eastern bank of Neawanna Creek in Seaside with bridges intact	18
Figure 4-3. Evacuation time at 4 fps to reach the lowest elevation point (earliest tsunami arrival) about 250 feet northeast of the base of Tillamook Head.....	19
Figure 4-4. Seaside evacuation opportunity map for the XXL1 (maximum-considered event covering ~100% of potential variability) tsunami scenario at 4 fps	20
Figure 4-5. Gearhart evacuation opportunity map for the XXL1 (maximum-considered event covering ~100% of potential variability) tsunami scenario at 4 fps	21
Figure 4-6. Simplified evacuation map showing only evacuation flow zones and direction arrows	22
Figure 5-1. Tsunami maximum flow depth map of Seaside for the maximum-considered XXL1, maximum-considered tsunami scenario.....	26
Figure 5-2. Tsunami maximum flow depth map of Seaside for the L1 or “Large” tsunami scenario.....	27
Figure 5-3. Tsunami maximum flow depth map of Gearhart for the maximum-considered XXL1, maximum-considered tsunami scenario.....	28
Figure 5-4. Tsunami maximum flow depth map of Gearhart for the L1 or “Large” tsunami scenario. Flow depth data are from Priest and others (2013a)	29

LIST OF TABLES

Table 2-1.	Speed conservation values used in modeling pedestrian evacuation difficulty in this study.....	4
Table 2-2.	Travel speed statistics for each travel speed group, compiled from travel speeds in the literature by Fraser and others (2014).....	11
Table 2-3.	Evacuation analysis maps in this study.....	12

LIST OF MAP PLATES

See the digital publication folder for files.

Plate 1.	Evacuation time map of Gearhart and Seaside the for maximum-considered XXL1 tsunami scenario at 4 fps
Plate 2.	Evacuation time map of Gearhart and Seaside for the L1 or “Large” tsunami scenario at 4 fps
Plate 3.	Evacuation time map of Seaside for the L1 tsunami scenario at 4 fps – Avenue G and Avenue U bridges out
Plate 4.	Evacuation time map of Seaside for the L1 tsunami scenario at 4 fps – Avenue A, West Broadway, and Highway 101 bridges out
Plate 5.	Evacuation time map of Seaside for the L1 tsunami scenario at 4 fps – hypothetical vertical evacuation structure at Seaside Civic and Convention Center
Plate 6.	Evacuation time map of Seaside for the L1 tsunami scenario at 4 fps – hypothetical vertical evacuation structure at Trendwest (WorldMark) Resort parking structure
Plate 7.	Tsunami wave advance map of Gearhart and Seaside for the maximum-considered XXL1 tsunami scenario
Plate 8.	Tsunami wave advance map of Gearhart and Seaside for the L1 tsunami scenario
Plate 9.	“Beat the wave” map for the maximum-considered XXL1 tsunami scenario for Seaside – all bridges intact and assuming a 5-minute evacuation delay
Plate 10.	“Beat the wave” map for the maximum-considered XXL1 tsunami scenario for Gearhart – all bridges intact and assuming a 5-minute evacuation delay
Plate 11.	“Beat the wave” map for the maximum-considered XXL1 tsunami scenario for Seaside – only retrofitted bridges intact (12th Street and 1st Avenue brides over the Necanicum River; 12th Street and Broadway Street over Neawanna Creek) and assuming a 5-minute evacuation delay
Plate 12.	“Beat the wave” map for the maximum-considered XXL1 tsunami scenario for Seaside – only retrofitted bridges intact (12th Street and 1st Avenue brides over the Necanicum River; 12th Street and Broadway Street over Neawanna Creek) and assuming a 10-minute evacuation delay
Plate 13.	“Beat the wave” map for the maximum-considered XXL1 tsunami scenario for Gearhart assuming a 10-minute evacuation delay

GEOGRAPHIC INFORMATION SYSTEM (GIS) DATA

See the digital publication folder for files.

Geodatabase is Esri® version 10.1 format. Metadata is embedded in the geodatabase and is also provided as separate .xml format files.

Seaside_Tsunami_Evacuation_Modeling.gdb:

Feature dataset: Evacuation_modeling_data

feature classes:

BTW_XXL1__AllBridgesIntact_5minDelay (polygon)
BTW_XXL1__RetrofittedBridgesOnly_5minDelay (polygon)
BTW_XXL1__RetrofittedBridgesOnly_10minDelay (polygon)
EvacuationRoutes_XXL1__AllBridgesIntact_HighResolution (polylines)
EvacuationRoutes_XXL1__AllBridgesIntact_LowResolution (polylines)
EvacuationRoutes_XXL1__RetrofittedBridgesOnly_HighResolution (polylines)
EvacuationRoutes_XXL1__RetrofittedBridgesOnly_LowResolution (polylines)

Raster data: Tsunami wave data

XXL1_MaximumTsunamiFlowDepth
XXL1_TsunamiWaveAdvance
L1_MaximumTsunamiFlowDepth
L1_TsunamiWaveAdvance

Metadata in .xml file format:

BTW-AllBridgesIntact_5minDelay.xml
BTW-RetroOnly_5minDelay.xml
BTW-RetroOnly_10minDelay.xml
EvacRoutes-AllBridgesIntact_HighRes.xml
EvacRoutes-AllBridgesIntact_LowRes.xml
EvacRoutes-RetroOnly_HighRes.xml
EvacRoutes-RetroOnly_LowRes.xml
FlowDepth-L1.xml
FlowDepth-XXL1.xml
WaveAdvance-L1.xml
WaveAdvance-XXL1.xml

ABSTRACT

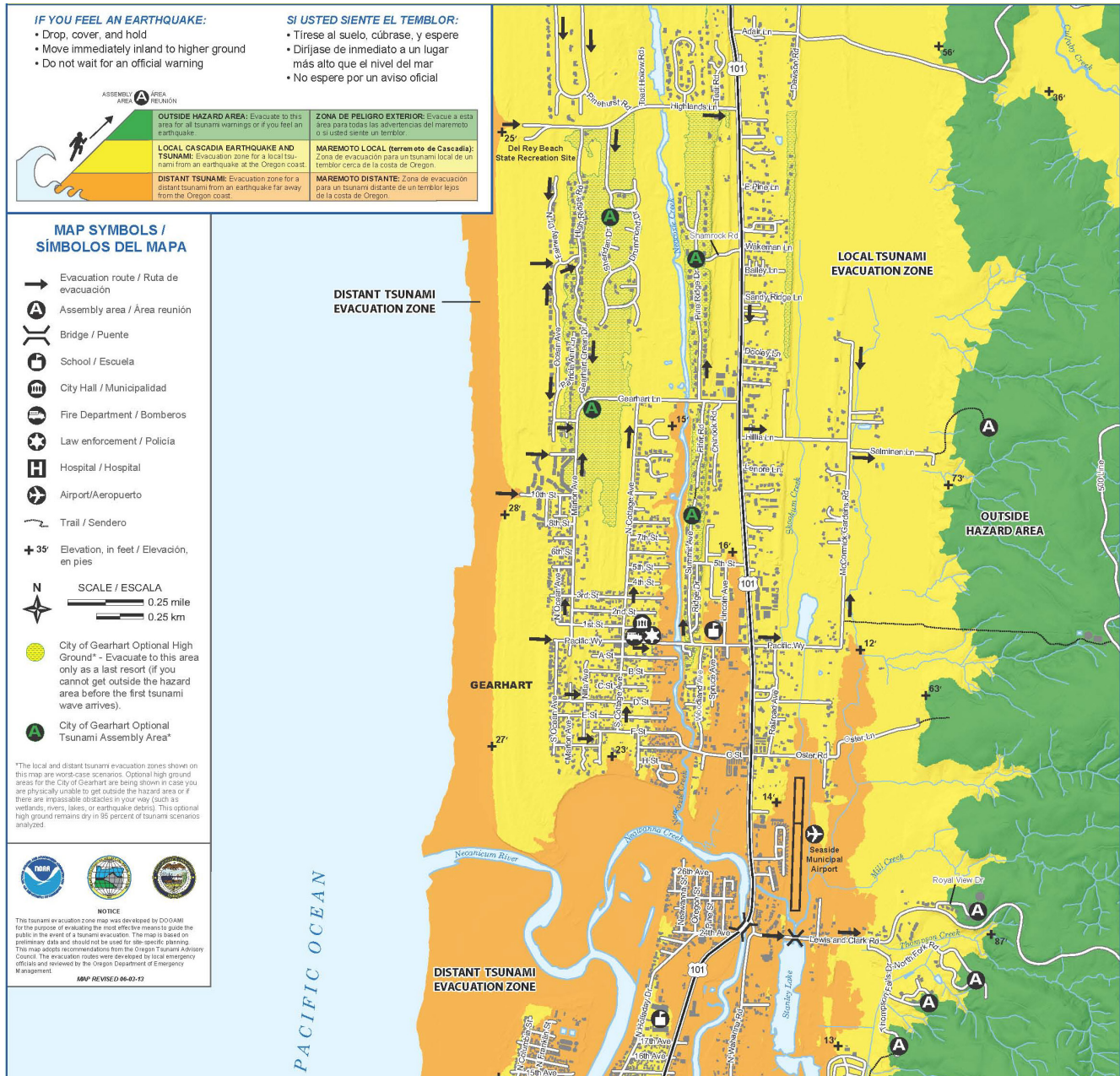
We evaluated difficulty of pedestrian evacuation of Seaside and Gearhart, Oregon, in the event of a local tsunami generated by an earthquake on the Cascadia subduction zone (CSZ). CSZ tsunami scenarios explored are 1) a maximum-considered event covering ~100% of potential variability, termed XXL1 and generated by a magnitude 9.1 earthquake, and 2) an event covering ~95% of variability, termed L1 and generated by a magnitude 9.0 earthquake. We determined minimum walking times to safety (within 20 ft of the inundation limit) for a moderate walking speed of 4 fps (22 minutes/mile) using least cost distance (LCD) routes determined by slight modification of the anisotropic path distance method of Wood and Schmidt (2012). Four feet per second is the standard speed for pedestrians to cross at signalized intersections. Evacuation was forced onto the roads and pedestrian pathways designated by local government reviewers as the most likely routes. In order to estimate whether pedestrians can stay ahead of a tsunami along entire routes, we produced tsunami wave advance maps for L1 and XXL1, a LCD walking time map (at 4 fps) to the east bank of the Necanicum River, a LCD map to the east bank of Neawanna Creek, a LCD map to the lowest point on the Tillamook Head evacuation route, and “beat-the-wave” (BTW) maps for the XXL1 scenario. The BTW maps depict minimum evacuation speed needed to stay ahead of the wave for three levels of increasing evacuation difficulty: 1) all bridges intact, 5-minute delay from start of earthquake before starting evacuation, 2) only retrofitted bridges intact, 5-minute delay, and 3) only retrofitted bridges intact, 10-minute delay. The results show that evacuation of Gearhart is challenging for a XXL1 tsunami but reasonably possible for an L1 event. Evacuation of Seaside seaward of the Necanicum River is extremely difficult for either the XXL1 or L1 scenario for those with mobility limitations (i.e., <4 fps). LCD and BTW trials showed that any failure of bridges greatly expands areas that cannot be evacuated at 4 fps. Possible

mitigation options include increasing the number of evacuation routes by construction of more earthquake-hardened bridges in Seaside, extending Salminen Lane in Gearhart, and installation of tsunami refuges, otherwise known as vertical evacuation structures. Although more bridges across the Necanicum River and Neawanna Creek in Seaside would increase evacuation efficiency, the area positively impacted by each additional bridge would be small relative to the area impacted by a tsunami refuge.

1.0 INTRODUCTION

A locally generated tsunami from a Cascadia subduction zone (CSZ) earthquake will inundate the Oregon coast within tens of minutes (Priest and others, 2009; Witter and others, 2011), making spontaneous evacuation on foot the only effective means of limiting loss of life, since vehicle evacuation would be quickly compromised by traffic congestion and road blockages. CSZ earthquakes affecting northern Oregon will likely be on the order of ~Mw 9.0 (Priest and others, 2009; Witter and others, 2011), severely damaging bridges and other infrastructure critical to evacuation. To evaluate CSZ tsunami impact, Witter and others (2011) used a logic tree approach to produce a suite of deterministic scenarios, five of which are mapped statewide, each covering the following percentages of potential variability of Cascadia tsunami inundation: XXL1 (100%), XL1 (98%), L1 (95%), M1 (79%), and SM1 (26%) (Priest and others, 2013b). In these scenarios a maximum-considered CSZ tsunami (XXL1) inundates virtually the entire area of Seaside and Gearhart, Oregon (Figure 1-1). The L1 tsunami inundates most of Seaside but leaves Gearhart with several large islands of high ground that greatly facilitate evacuation (Figure 1-1). Further complicating evacuation in Seaside is heavy reliance of evacuation routes on bridges crossing the Necanicum River and Neawanna Creek (Figure 1-1).

Figure 1-1. Portion of DOGAMI (2013) tsunami evacuation map for Seaside-Gearhart showing geographic information; inundation for Cascadia subduction zone (CSZ) tsunami scenario XXL1 (yellow and orange areas), a maximum-considered event; ground outside the XXL1 hazard area (green area); and in the green the hatched area, localities in Gearhart below XXL1 inundation but above inundation of CSZ tsunami scenario L1 (an event covering ~95% of potential CSZ tsunami variability); see Witter and others (2011) for detailed explanations of all tsunami scenarios depicted on this map.



The objective of this study is to provide local government with a quantitative assessment of the difficulty of evacuating Seaside and Gearhart for the XXL1 and L1 scenarios in order to evaluate mitigation options such as evacuation route improvement, better wayfinding, land use planning actions, and implementation of vertical evacuation. We achieve the objective by 1) using the least cost distance (LCD) approach of Wood and Schmidtlein (2012) to provide estimates of walking times to safety, here defined as 20 feet beyond the inundation zone, for every place of origin in the community, 2) illustrating how quickly the wave front of an L1 or XXL1 tsunami advances across the area after the causative earthquake, and 3) determining whether an evacuee can stay ahead of the tsunami all the way to safety on the routes defined by the LCD analysis. The latter method is implemented by a new approach termed “beat-the-wave” (BTW) evacuation difficulty analysis that shows minimum speed to stay ahead of the tsunami all the way to safety.* We then summarize which parts of each city are most in need of tsunami hazard mitigation.

2.0 METHODS

Agent-based and LCD modeling are the two most common approaches for simulating pedestrian evacuation difficulty. Agent-based modeling focuses on the individual and how travel would most likely occur across various cost conditions, such as congestion points (Yeh and others, 2009). LCD modeling focuses on characteristics across the evacuation landscape, such as slope and land cover type. LCD modeling calculates a least-cost path to the tsunami inundation limit for every point in the inundation zone. Time to traverse a route can then be estimated from a pedestrian walking speed for optimal conditions (e.g., a flat paved street), increasing or decreasing that speed for slope and other ground conditions. We used the LCD model of Wood and Schmidtlein (2012) because we wanted to understand the spatial distributions of evacuation times across the

region of Seaside and Gearhart, Oregon, without having to create a large number of scenarios for specific starting points required by agent-based models. We assumed a pedestrian walking speed of 4 feet per second (fps) [22 minute/mile; 1.22 meters/second], listed as a moderate walk by Wood and Schmidtlein (2012). This is the speed generally required to cross from curb to curb at signalized intersections (Langlois and others, 1997; U.S. Department of Transportation, 2012).

LCD modeling is based on a cost raster, where each pixel represents a level of difficulty of movement across the surface. In the Wood and Schmidtlein (2012) approach these difficulty or cost values are categorized as *speed conservation values* (SCV), where each value is representative of the land cover type across the landscape. Land cover SCVs adjust the base travel speed using terrain-energy coefficients discussed by Soule and Goldman (1972), including “No Data” to note where travel is not allowed (e.g., over water, through fences or buildings, and most natural areas for this case study). The base travel speed assumes constant energy expenditure. Geospatial data representing roads, pedestrian paths and backshores were generated through manual classification of imagery, field verified and then reviewed by local officials.

At the urging of local government and technical reviewers, we used a model that considered only roads, paths, and the dry sand backshore of beaches as evacuation pathways; all other land cover classes were essentially excluded. The backshore is defined as areas landward of the beach-dune junction approximated by the 18-ft NAVD88 contour. The beach (below 18 ft) was excluded owing to uncertainty of travel difficulty (cost) on wet versus dry sand and potentially liquefied sand during a local subduction zone earthquake. We chose to ignore travel time from buildings or other parts of urban areas to the roads, because there is large uncertainty in conditions both before (e.g., fenced yards) and after the earthquake (e.g., fallen debris). The modeling approach thus produces minimum evacuation times. To force the model to use only these routes, we used the SCV values presented in [Table 2-1](#).

*This report was produced in tandem with an abbreviated version submitted to *Natural Hazards* (Priest and others, 2015) that summarizes only the BTW approach applied to Seaside.

In coastal towns, landslide-prone slopes and saturated sandy soil are common, so slides, liquefaction, and lateral spreading are likely to occur during an earthquake. These hazards will damage roads and reduce walking speeds by significant but uncertain amounts. Although it is possible to model potential distribution of these hazards for Seaside and Gearhart, that was beyond the scope of this study. Even if mapped, assigning cost values to these hazard areas is highly uncertain, since actual slowing of pedestrian speed will likely be highly site specific.

We implemented LCD modeling by using Esri ArcGIS® 10.1 software. The path distance tool uses geospatial algorithms to calculate the most efficient route from each point in the evacuation zone to

“safety,” defined for the purposes of this study as within ~20 feet of the maximum inundation limit; this is where the tsunami flow depth and velocity are effectively zero. The safety destination was created by applying a buffer of 20 feet (6 m) on each side of the inundation boundary polyline (derived from the seaward margin of dry computational points in the tsunami simulation) and converting this into a raster data file. This raster file was created as a proxy for the inundation boundary to avoid breaks in the boundary created when the coarseness of the grid spacing causes two adjacent raster pixels to meet only at their adjoining corner points. [Figure 2-1](#) summarizes the steps and inputs into the path distance tool.

Table 2-1. Speed conservation values used in modeling pedestrian evacuation difficulty in this study.

Feature Type	Speed Conservation Value*
Roads	1
Beach access pathways	0.5556**
Everywhere else	0

*Speed conservation values (SCV) are derived from Wood and Schmidtlein (2012).

**Beach access pathways have the same SCV as sand given by Wood and Schmidtlein (2012).

2.1 Tsunami hazard zone layers

The two tsunami inundation zones used in this study are L1 and XXL1 derived from digital data of Priest and others (2013a,b). These two zones cover, respectively, about 95 and 100 percent of potential CSZ inundation (Witter and others, 2011).

2.2 Lidar elevations layer

We created digital elevation models (DEMs) by interpolating lidar (laser-based mapping) points into a 1-ft-resolution raster and using the highest hit data rather than ground or water surface data where there were bridges. As modeling proceeded, we realized that this approach introduced significant error. The lidar data have a native vertical accuracy on bare pavement of 2-3 inches. When calculating slopes using a 1-foot cell, 2-3 inches of elevation noise results in a noisy

slope profile and introduces slope artifacts of significant amplitude (e.g., a 3-inch elevation difference between cells 1 foot apart makes a 14 degree slope). [Figure 2-2a](#) and [Figure 2-2b](#) illustrate these artifacts. The LCD model is very sensitive to slope, and the maximum speed is reached at slopes of about –3 degrees; steeper negative slopes actually slow progress. This means that the slope noise introduced by fine-scale sampling of the lidar DEM added significantly more time to the total calculated time. To smooth the data, we created points at 50-foot intervals along all evacuation paths including major roads and at intersections and attributed those points with elevation values from the native 3-foot-cell lidar DEM. In trials at 25, 50, and 100 feet, 50 feet achieved the best compromise between accuracy and smoothness. Final sampling interval was ~50 feet on straight paths and somewhat less for curved paths in order to accurately depict curvatures. We then

interpolated those points using an Esri Natural Neighbor function to produce a smoothed DEM that closely captured the actual elevation values of the lidar while dramatically reducing slope noise (Figure 2-2c).

Figure 2-1. Model diagram of path distance approach from Wood and Schmidtlein (2012). SCV is speed conservation value, DEM is digital elevation model.

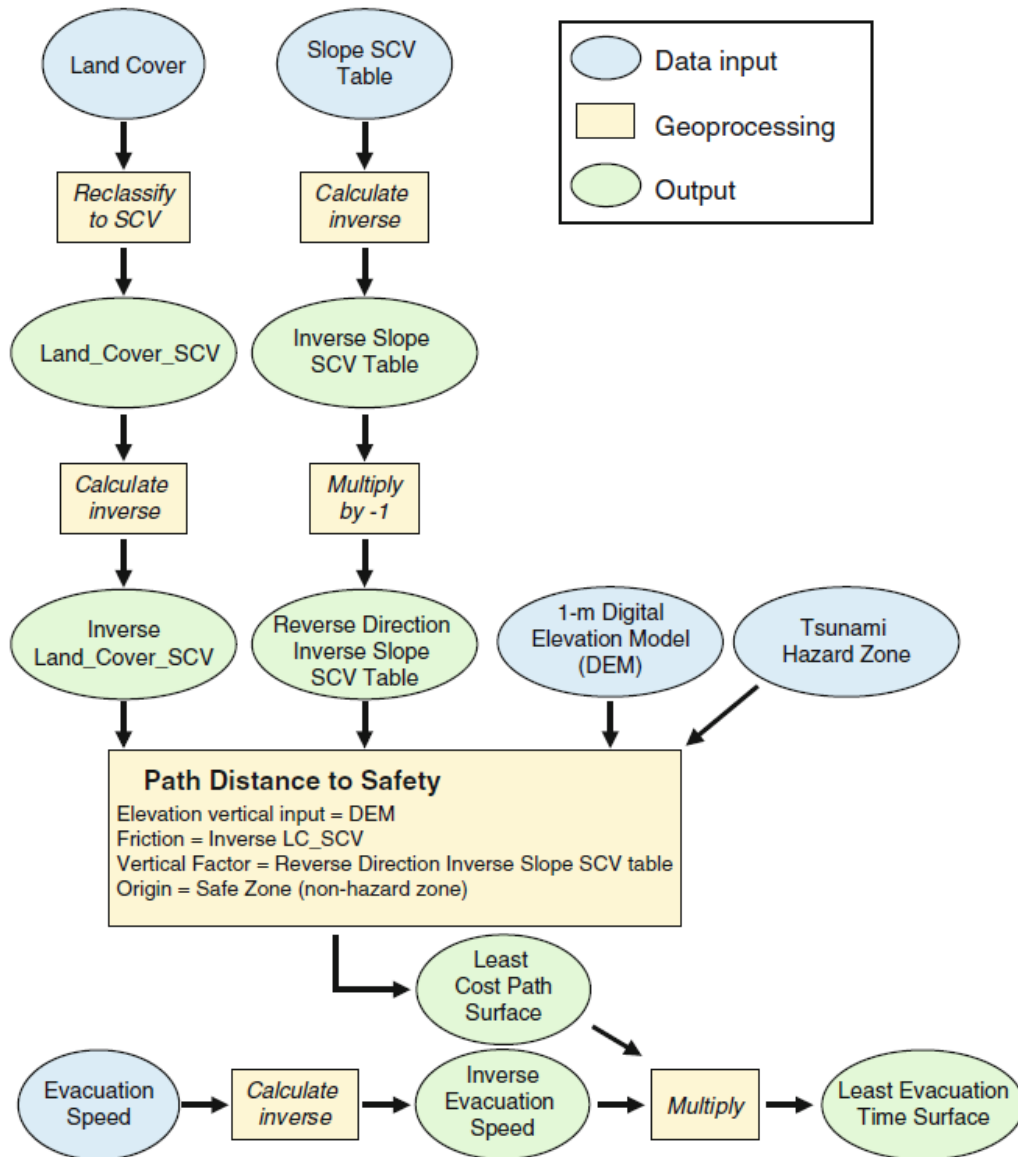
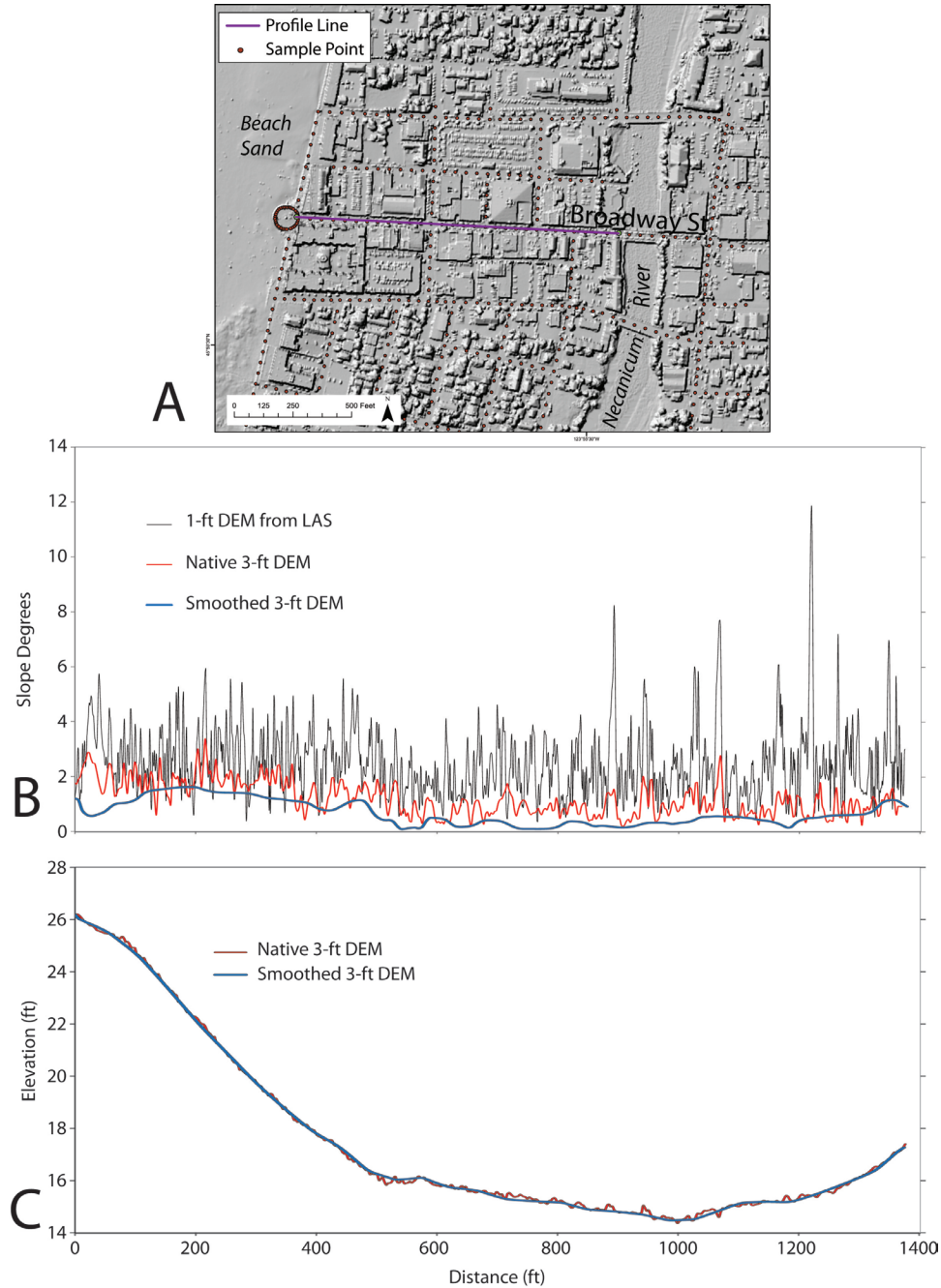


Figure 2-2. Calculation of slope along Broadway Street. A) Location map for profile along Broadway Street in Seaside of smoothed digital elevation model (DEM) showing location of elevation sample points used. B) Comparison of slope along the Broadway profile between the 1-ft DEM made from lidar points, the native 3-ft (0.9-m) DEM, and the smoothed 6-ft (1.8-m) DEM. Both the 1-ft and 3-ft DEMs have large amounts of slope noise that would cause the least-cost-distance (LCD) model to return artificially long evacuation times and effective distances. The smoothed DEM was made by natural neighbor interpolations of elevations from the native 3-ft DEM sampled at the 50-ft (15-m) intervals shown in A. C) Comparison of the elevations from final smoothed DEM to the native 3-ft (0.9-m) DEM. The smoothed DEM closely matches the native elevation, resulting in significantly less slope noise. DEM for the map and cross sections is from 2009 lidar data.



2.3 Speed Conservation Value (SCV) slope table

We created a table that associates slopes with a specific SCV value. This table used the same values as those of Wood and Schmidtlein (2012), and, as in their approach, we estimated the effect of slope on speed from Tobler's (1993) hiking function:

$$\text{walking speed (km/hr)} = 6e^{-3.5 \times \text{abs}(\text{slope} + 0.05)}$$

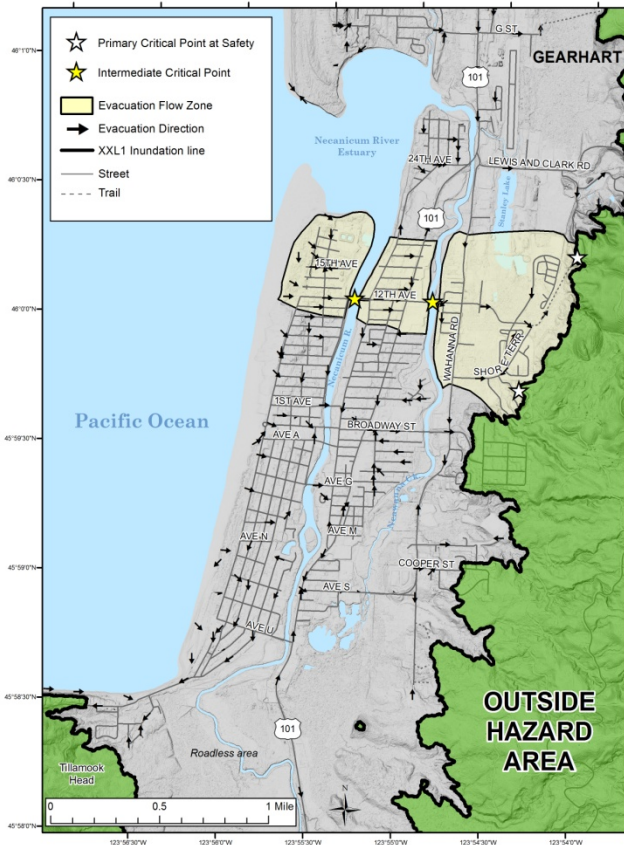
where slope is equal to the tangent of the slope angle. This formula is based on empirical data of Imhof (1950) and predicts that speed is fastest on gentle (–5%) downslopes.

The output of the LCD model is a path distance surface showing the effective path length to safety from each pixel. We also calculated an LCD backlink raster which shows, for each cell, the direction of the next cell on the least-cost path. This raster makes it possible to trace the path to safety from any pixel and is equivalent to a flow direction raster, which is the first step in hydrologic modeling of topographic surfaces. We use the hydrologic tools in ArcGIS 10.1 and the backlink raster to extract a “stream” network to visualize the paths used for most efficient evacuation (**Figure 2-3**). These paths represent the shortest effective distances to safety. The pixel value for cost distance is the effective distance, along the least-cost path, from the pixel to the point where the path intersects safety. The resulting direction of travel on each path is depicted by the GIS software as arrows along streets with opposing arrows where one could travel to safety on two equal alternative paths. The latter define boundaries of evacuation flow toward critical points such as bridges and are directly analogous to watershed boundaries or drainage divides in hydrologic modeling (**Figure 2-3**). These boundaries are particularly important in Seaside, where one must choose which bridge to evacuate

across from each part of town. At typical map scales, the large number of arrows output by the software can be hard to decipher and can obscure the evacuation flow zones, so depicting the zones on hazard maps as in **Figure 2-3** is recommended.

At the urging of local government reviewers, we also produced LCD maps for the L1 scenario in Seaside showing the effect of two different vertical evacuation options, and collapse of some bridges not retrofitted to withstand a Cascadia subduction zone earthquake. As of the date of this publication, the only bridges designed to withstand significant seismic forces are the 1st Avenue Bridge across the Necanicum River, the Broadway Street bridge across Neawanna Creek, and the two 12th Avenue bridges across both (Kevin Cupples, personal communication, 2014). Local government reviewers also requested LCD maps depicting walking times to the east bank of the Necanicum River, the east bank of Neawanna Creek, and the lowest elevation point near the base of Tillamook Head in order to compare tsunami arrival times to pedestrian arrival (at 4 fps) at these critical points. As we constructed these maps, it became apparent that many more would be needed to fully explore an array of evacuation speeds appropriate for specific populations (e.g., elderly versus able-bodied adults). In the next section we explore a way of solving this problem by producing tsunami wave front advance maps and integrating tsunami wave arrival data directly into the LCD analysis to produce “beat-the-wave” (BTW) maps that estimate the minimum speed needed to reach safety ahead of the wave. The estimates of time to reach critical points at 4 fps on LCD maps are still useful, since they factor in the slowing over difficult terrain, whereas the BTW approach outlined below uses only geographic distance to safety to calculate minimum needed speeds, albeit terrain factors do constrain optimal paths to safety.

Figure 2-3. Example of the network of least-cost paths from the least-cost-distance (LCD) analysis limited to trails and streets. Evacuation flow zones are illustrated for the 12th Avenue evacuation route. Evacuation flow is landward through intermediate critical points at bridges to the primary critical point at safety. Base map boundary on this and following figures is shaded relief from 2009 lidar data; XXL1 inundation boundary on this and following figures is from Priest and others (2013b).



2.4 Beat-the-Wave (BTW) Modeling

BTW models integrate tsunami wave arrival data directly into the LCD analysis to produce a map of minimum speeds that must be maintained to reach safety. In order to understand the complexities of tsunami wave advance across the landscape, we extracted the time after the CSZ earthquake at which the XXL1 tsunami flow depth reached more than 0.5 ft at each computational grid point and interpolated those arrival data to create a continuous map (Figure

2-4, Plate 7) and examined profiles of the data on LCD paths (Figure 2-5); we also produced a wave front advance map for the L1 scenario as an ancillary map product (Plate 8). We then determined when the XXL1 tsunami water elevation reached the bottom of bridge spans, considering that the most likely time bridges might be compromised by the full hydraulic force of the tsunami (Figure 2-5). The map and profiles illustrate that the tsunami races up the shore-parallel waterways, reaching bridges before overland inundation can reach the same bridges (Figure 2-5). Likewise, overland inundation is fastest at the lowland on the south end of town (Figure 2-5), so any evacuation south to Tillamook Head would need to beat the wave to the lowland at the base of that headland. Each of these early arrival points creates an intermediate, secondary critical point before the primary critical point at safety.

The next step in BTW analysis is to determine optimal geographic distances to safety from every grid point by employing the path distance tool. If evacuation flow zones and directions established by LCD matched flow zones resulting from this geographic path distance analysis, and there were no complications from early tsunami arrivals inland of the shoreline, the analysis of minimum path distance would be complete at this step. However, the LCD flow zone boundaries will generally be slightly different from boundaries resulting from the geographic path distance analysis, and speeds may need to be increased to beat the tsunami to secondary critical points (Figure 2-5). We forced the path distance analysis to abide by the LCD flow zone boundaries and the intermediate critical points by running separate analyses of geographic distances to critical points within each LCD flow zone to each critical point destination. The resulting output raster files are the shortest distances within each flow zone or “watershed” to these points from every part of the study area. This step is accomplished by trimming the grid to each LCD flow zone boundary and running the geographic path distance analysis for each one. At this point we had within each of the flow zones the minimum geographic path distance for all pixels to every intermediate and primary critical point.

The final step in calculating the time available for evacuation is subtracting time from the simulated tsunami arrival times after the causative earthquake to account for delay in evacuation start. Using the March 11, 2011 Tohoku earthquake (USGS, 2012) as an analogue to an XXL1 or L1 scenario, the minimum delay is probably ~3–5 minutes of strong shaking for the ~Mw 9.0 event. There are little empirical data on how long it takes people to begin evacuation after shaking, but Mas and others (2013) found in 2010 and 2011 surveys a mean of 7 minutes to start at La Punta, Peru which had experienced several local earthquakes and tsunamis over the last ~400 years, the last being in 1974. We simulated 2 scenarios, a delay of 5 minutes mainly for earthquake shaking, and a delay of 10 minutes (the minimum of 3 minutes for shaking plus 7 minutes based on the La Punta survey). We also examined the effect of bridge collapse, running trials with all bridges intact and only seismically retrofitted bridges, giving a set of three scenarios with increasing evacuation difficulty: 1) all bridges intact, 5-minute delay from start of earthquake before starting evacuation, 2) only retrofitted bridges intact, 5-minute delay, and 3) only retrofitted bridges intact, 10-minute delay.

Actual travel speeds on any path will require either variable expenditure of energy to maintain the BTW speed in all conditions or higher speeds in easier terrain (flat paved streets) to compensate for slowing in difficult terrain (steep slopes or sand). Users should

be advised about these practical issues in the map explanation.

Binning of evacuation speeds was limited to five categories, which is typically the maximum number that the public can easily interpret on a map. A literature review of typical pedestrian speeds by Fraser and others (2014) found five travel speed groups: elderly, child, adult impaired, adult unimpaired, and running (**Table 2-2**). The ranges of speeds for these groups at one standard deviation (i.e., the last two rows of **Table 2-2**) provide some guidance for establishing bins that would be useful on the BTW map. Speed categories in the map explanation were then given qualitative names such as “slow walking” and “running” so the public can relate speed bins to their experience. Of particular interest are groups that will be most vulnerable, such as impaired adults and the elderly with mean speeds of 3 fps and a range of ~2–4 fps (**Table 2-2**). After looking at the range of BTW speeds for Seaside and reviewing a number of references describing speed categories (Paul, 2013; Margaria, 1938), we used the following five speed bins to capture the natural boundaries between pedestrian speeds based on mode of locomotion and the speed group most applicable to each bin: Very slow walking at 0–2 fps, slow walking at 2–4 fps for elderly and impaired adults, walking at 4–6 fps for unimpaired adults, fast walking to slow jogging at 6–8 fps for fit adults, and running at >8 fps.

Figure 2-4. Illustration of XXL1 tsunami arrival times after a Cascadia subduction zone earthquake showing locations of three evacuation routes at Seaside. Detailed profiles of arrivals at each route are given in Figure 2-5.

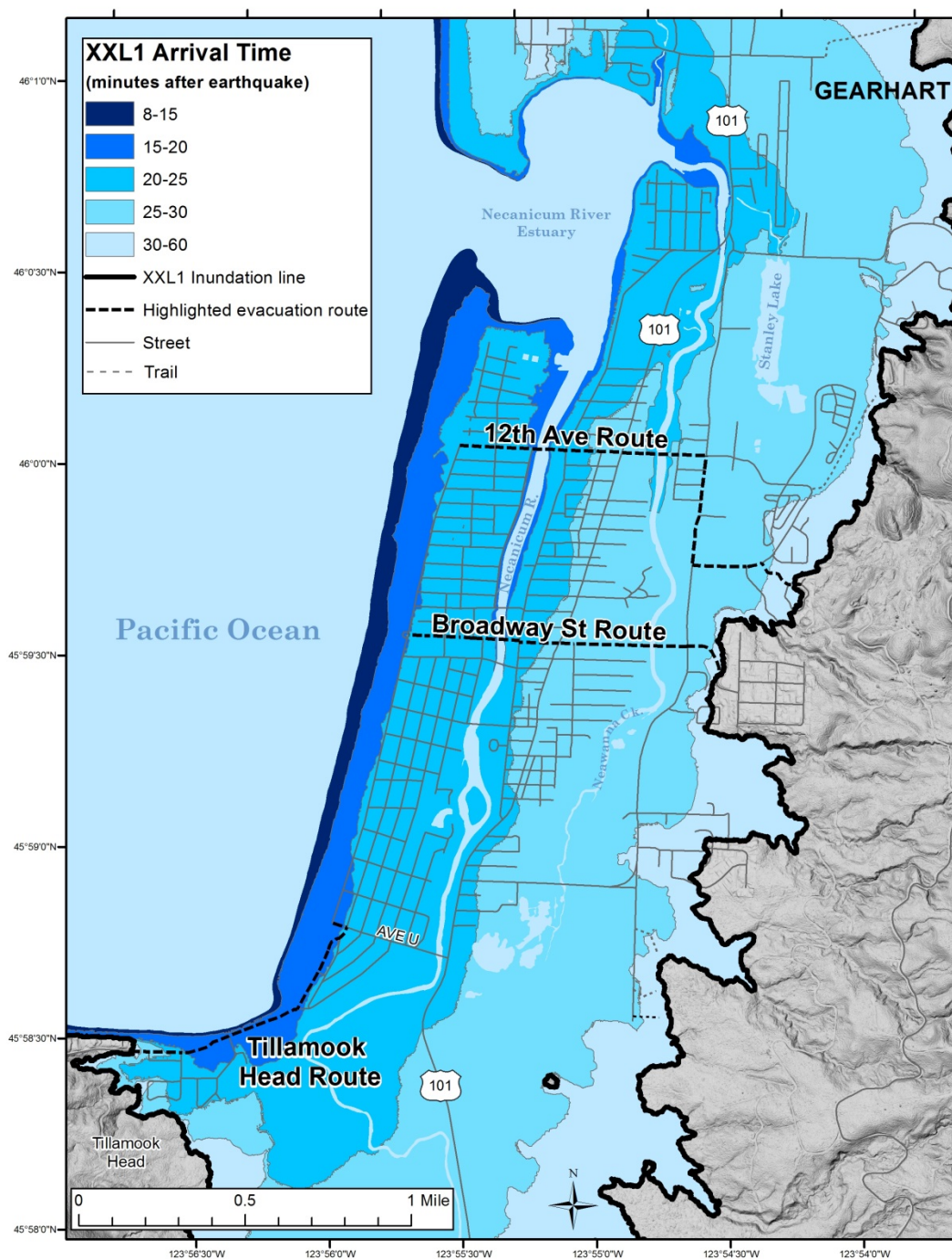


Figure 2-5. XXL1 times after the earthquake when simulated tsunami flow depth exceeded 0.5 ft for each evacuation route shown on the map of Figure 2-4. Bridge arrivals are the times when the tsunami reaches the bottom of each bridge. Early arrivals at the Necanicum River bridge, Neawanna Creek bridge, and near the base of Tillamook Head are critical points setting the times for evacuation for the entire evacuation flow zone seaward of each point. In BTW mapping the tsunami arrival times are reduced by 5 minutes to account for a delay in evacuation from effects of earthquake shaking.

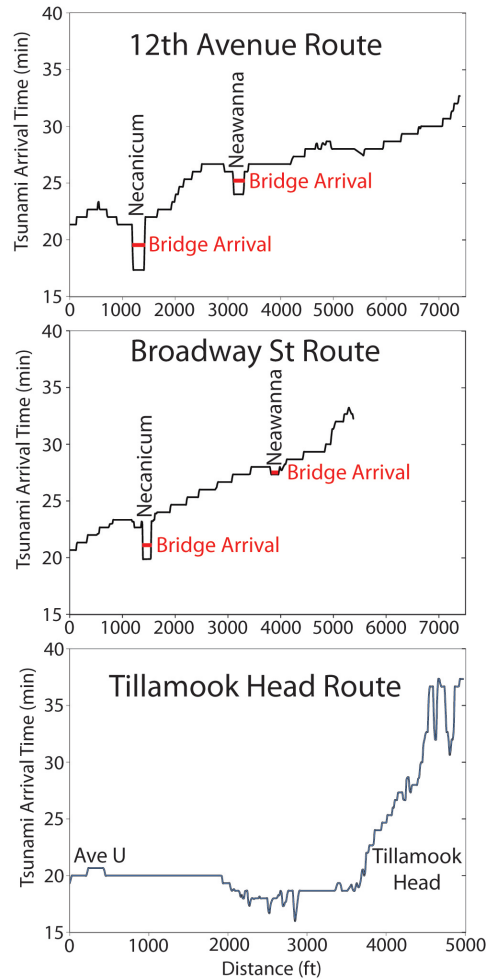


Table 2-2. Travel speed statistics for each travel speed group, compiled from travel speeds in the literature by Fraser and others (2014). SD is standard deviation.

	Adult Impaired	Adult Unimpaired	Child	Elderly	Running
Minimum	1.9 fps	2.9 fps	1.8 fps	0.7 fps	5.9 fps
Maximum	3.5 fps	9.2 fps	6.9 fps	4.3 fps	12.6 fps
Mean	2.9 fps	4.7 fps	4.2 fps	3.0 fps	9.1 fps
SD	0.6 fps	1.6 fps	2.6 fps	1.0 fps	3.3 fps
Mean + SD	3.5 fps	6 fps	7 fps	4 fps	12 fps
Mean – SD	2 fps	3 fps	2 fps	2 fps	6 fps

Table 2-3. Evacuation analysis maps in this study; n/a = not applicable; fps is feet per second; XXL1 is the maximum-considered tsunami event covering ~100% of potential variability; L1 is an event covering ~95% of variability.

Figure or Plate	Type of Analysis	Evacuation Destination	Bridges That Fail	Vertical Evacuation Site	Evacuation Delay from Start of Earthquake (minutes)
Figure 7	evacuation time at 4 fps	east bank Necanicum River	none	none	n/a
Figure 8	evacuation time at 4 fps	east bank Neawanna Creek	none	none	n/a
Figure 9	evacuation time at 4 fps	XXL1 hazard zone boundary at Tillamook Head	none	none	n/a
Figure 10	evacuation opportunity at 4 fps for Seaside	XXL1 hazard zone boundary	All but the 12th Ave., bridges, 1st Ave. Bridge across the Necanicum River, and the east Broadway St. bridge across Neawanna Creek	none	5
Figure 11	evacuation opportunity at 4 fps for Gearhart	XXL1 hazard zone boundary	All but the 12th Ave., bridges, 1st Ave. Bridge across the Necanicum River, and the east Broadway St. bridge across Neawanna Creek	none	5
Plate 1	evacuation time at 4 fps for Gearhart and Seaside	XXL1 hazard zone boundary	none	none	n/a
Plate 2	evacuation time at 4 fps for Gearhart and Seaside	L1 hazard zone boundary	none	none	n/a
Plate 3	evacuation time at 4 fps for Seaside	L1 hazard zone boundary	Avenues G and U	none	n/a
Plate 4	evacuation time at 4 fps for Seaside	L1 hazard zone boundary	Avenue A, West Broadway, Highway 101	none	n/a
Plate 5	evacuation time at 4 fps for Seaside	L1 hazard zone boundary	none	Seaside Civic and Convention Center	n/a
Plate 6	evacuation time at 4 fps for Seaside	L1 hazard zone boundary	none	Trendwest Resort parking structure	n/a
Plate 7	tsunami wave advance for Gearhart and Seaside	XXL1 hazard zone boundary	none	none	n/a
Plate 8	tsunami wave advance for Gearhart and Seaside	L1 hazard zone boundary	none	none	n/a
Plate 9	"Beat the wave" map for Seaside	XXL1 hazard zone boundary	none	none	5

Figure or Plate	Type of Analysis	Evacuation Destination	Bridges That Fail	Vertical Evacuation Site	Evacuation Delay from Start of Earthquake (minutes)
Plate 10	"Beat the wave" map for Gearhart	XXL1 hazard zone boundary	none	none	5
Plate 11	"Beat the wave" map for Seaside	XXL1 hazard zone boundary	All but the 12 th Ave., bridges, 1st Ave. bridge across the Necanicum River, and the east Broadway St. bridge across Neawanna Creek	none	5
Plate 12	"Beat the wave" map for Seaside	XXL1 hazard zone boundary	All but the 12th Ave., bridges, 1st Ave. bridge across the Necanicum River, and the east Broadway St. bridge across Neawanna Creek	none	10
Plate 13	"Beat the wave" map for Gearhart	XXL1 hazard zone boundary	All but the 12th Ave., bridges, 1st Ave. bridge across the Necanicum River, and the east Broadway St. bridge across Neawanna Creek	none	10

The final procedure is summarized as follows (Priest and others, 2015):

1. Run the standard LCD analysis of Wood and Schmidtlein (2012) to the inundation boundary to establish evacuation flow zone boundaries.
2. Extract times that tsunami flow depth reaches more than 0.5 ft (15 cm) at each computational grid point and when the tsunami reaches the bottom of bridge spans.
3. Subtract from the tsunami arrival times anticipated delay of evacuation from earthquake shaking and behavioral factors.
4. Note tsunami arrival times at primary critical points (at the inundation boundary) and at intermediate (secondary) critical points where there are early tsunami arrivals such as route crossings at bridges or low points. These are the times to evacuate flow zones seaward of these points.
5. Determine the minimum distance from every grid cell to the inundation boundary (primary critical points) by running the path distance algorithm using only the surface distance (i.e., leaving out the land cover cost raster and the vertical cost factor defined by the slope in the standard LCD analysis).
6. Determine the minimum distance from every grid cell to each secondary critical point by running the path distance algorithm using only on the surface distance.
7. Trim each raster file output from step 6 to the flow zone of Step 1 that is appropriate for (seaward of) that critical point. Alternatively, one could trim the input grid to the appropriate flow zone before running Step 6; this would save some computational time.
8. Divide the least cost distances in all raster files of steps 5 and 7 by the appropriate primary or secondary critical point tsunami arrival times (step 4) appropriate for each flow zone.
9. Mosaic all of the speed raster files from step 8 by selecting for the maximum speed at each grid cell. The result is a raster map of minimum speed that must be maintained over the entire evacuation path from each grid cell to reach safety ahead of the advancing tsunami wave.

3.0 RESULTS

We evaluated evacuation difficulty of Seaside and Gearhart by producing these maps (**Table 2-3**):

- Evacuation times to safety given a walking speed of 4 fps (Plates 1–6)
- Tsunami wave advance showing first arrival of scenario tsunamis L1 and XXL1 (Plates 7 and 8)
- Evacuation time at 4 fps to the east bank of the Necanicum River (**Figure 4-1**)
- Evacuation time at 4 fps to the east bank of Neawanna Creek (**Figure 4-2**)
- Evacuation time at 4 fps to the lowest elevation point on the evacuation path to Tillamook Head (**Figure 4-3**)
- Evacuation opportunity maps produced by binning BTW values at greater than and less than 4 fps for the XXL1 tsunami scenario at Seaside (**Figure 4-4**) and Gearhart (**Figure 4-5**) (as a way to relate BTW maps to the standard evacuation time maps). We chose as an example the BTW scenario with 5-minutes delay in evacuation, only retrofitted bridges intact.
- BTW maps for the XXL1 tsunami scenario with all bridges intact, 5-minute evacuation delay (Plates 9 and 10); only seismically retrofitted bridges intact with a 5-minute evacuation delay (Plate 11) and 10 minute delay (Plates 12 and 13).

When the project began prior to development of the BTW approach, local government officials in Seaside requested estimates of walking times at 4 fps to the Necanicum River (**Figure 4-1**) and Neawanna Creek (**Figure 4-2**) bridges, and to the lowest point on the evacuation path near the base of Tillamook Head (**Figure 4-3**). These maps were requested to better understand whether these secondary critical points could be reached before wave arrival. While we did produce these maps, we developed the evacuation opportunity and BTW methods to provide an easier means of answering the questions than comparing tsunami wave advance maps and single-speed evacuation time maps. **Figure 4-4** and **Figure 4-5** illustrate evacuation opportunity maps for Seaside and Gearhart, respectively, for the XXL1 tsunami assuming a 5-minute evacuation delay and only

seismically retrofitted bridges intact. Plates 9 and 10 illustrate BTW maps for the XXL1 scenario for the same scenario, while two additional BTW maps for Seaside illustrate how much faster one must go if only retrofitted bridges survive (Plate 11) and evacuation is delayed 10 minutes (Plate 12). Evacuation times at 4 fps for much of the seaward part of the study area are problematic, particularly if evacuation cannot begin until about 5-10 minutes after start of the earthquake. Even with all bridges intact after an earthquake, LCD analysis of evacuation times at 4 fps illustrate that much of western Seaside is close to the 33- to 35-minute XXL1 and L1 tsunami arrivals at the respective inundation limits (Plates 1 and 2). Evacuees in western and southern Gearhart would be unable to reach safety for XXL1 at 4 fps (Plates 1 and 7; **Figure 4-5**). Evacuation times at 4 fps for the L1 tsunami in Gearhart are also problematic for areas near the beach, but most evacuees in Gearhart could reach safety (compare Plates 2 and 8). The maps of walking time at 4 fps to secondary critical points on the way to safety (**Figure 4-3**, **Figure 4-4** and **Figure 4-5**) illustrate similar challenges. For example, evacuation at 4 fps of the Seaside beaches is problematic before a local XXL1 tsunami floods to the underside of Necanicum River bridges at 19–21 minutes (compare **Figure 2-5** to **Figure 4-1**). Furthermore, the LCD paths to safety at Tillamook Head from Avenue L to Avenue T (Plates 1 and 2) will be cut off by the XXL1 tsunami arrival at ~16–18 minutes in the low ground near the base of Tillamook Head (**Figure 2-5** and **Figure 4-3**); hence, only those evacuating from southwest of approximately Avenue S are likely to reach safety at the headland when a 5-minute delay of evacuation is factored in (**Figure 4-4**).

Estimates of needed speed to “beat the wave” for the XXL1 scenario (**Figure 4-4** and **Figure 4-5**; Plates 9-11) illustrate that those with limited mobility like the elderly with estimated speeds of 2-4 fps will have great difficulty evacuating western Seaside and Gearhart. Even with all bridges intact and only a 5-minute evacuation delay, evacuees in large parts of western Seaside and Gearhart must maintain speeds of 2–4 fps all the way to safety, even though that can be as much as a mile away (Plate 9). Speeds of 4–6 fps

would be necessary to evacuate the most distal area in this best case scenario (Plate 9). If non-retrofitted bridges fail, then the amount of Seaside that cannot be evacuated at the 2–4 fps increases substantially (Plate 11). Even able-bodied adults able to walk 4–6 fps would have great difficulty evacuating local areas seaward of the Necanicum River if vulnerable bridges fail and there is 10 minutes evacuation delay from the start of the earthquake (Plate 12). The L1 tsunami arrival times in much of Seaside are nearly the same as XXL1 (compare Plates 7 and 8), so these findings for Seaside apply to that scenario as well.

Comparing the wave advance map for L1 (Plate 8) to the L1 evacuation time maps at 4 fps (Plates 2–4) illustrates relative sensitivity of evacuation difficulty to various bridge failures and to construction of tsunami refuges. Removing the Avenue G and U bridges in Seaside only slightly increases the area of problematic evacuation (Plate 3). Removing the Avenue A, West Broadway, and Highway 101 bridges severely compromises evacuation in the northern part of Seaside west of the Highway 101 bridge but has only modest effects elsewhere (Plate 4). Adding vertical evacuation at either the Seaside Civic and Convention Center (Plate 5) or the Trendwest Resort parking structure (Plate 6) greatly enhances evacuation in westernmost Seaside, provided such structures have capacity adequate for the projected number of evacuees.

4.0 DISCUSSION

4.1 Key findings

By depicting minimum speeds to reach safety from every part of a study area, the BTW approach to evacuation difficulty analysis accomplishes in a single map what would take many maps using a single evacuation speed to estimate evacuation time (e.g., Wood and Schmidtlein, 2012). Unlike the single speed approach, BTW analysis takes into account early tsunami arrivals at waterways and lowlands that can catch evacuees before reaching safety. Examination of the tsunami wave front advance across the study area is a critical first step in identifying where the tsunami may arrive early along some routes relative to what

would be expected for normal dry land inundation. For example, in Seaside the tsunami races up shore-parallel waterways, arriving at bridges before the landward advancing wave strikes these same bridges (Figure 2-4 and Figure 2-5). Likewise, overland flooding happens much faster at a low point on the south side of town, cutting off southward evacuation to the nearby highland at Tillamook Head (Figure 2-4 and Figure 2-5). Minimum speeds to safety must be adjusted upward to make sure that these critical points can be crossed by those evacuating toward them. We illustrate a method of doing this adjustment using standard LCD (least cost distance) and mosaicking tools in ArcGIS. The final BTW maps depict with arrows and evacuation flow zones the most efficient evacuation routes. Evacuation flow zone boundaries are particularly useful because they clarify evacuation routes (i.e., which bridges to cross) and depict break points between two equally efficient routes to safety. Flow zones and the direction arrows provide valuable guidance, even without the BTW speed information (Figure 4-6).

The Wood and Schmidtlein (2012) single speed approach is really aimed at answering a simple question: which parts of a community can and cannot be evacuated at a single nominal walking speed for unimpaired adults such as 4 fps? The BTW map can answer that question definitively by binning output into greater or less than 4 fps. The resulting evacuation opportunity map provides the yes-no answer at a glance (Figure 4-4 and Figure 4-5).

Plates 9 and 10 show that much of the study area can be evacuated to safety for a maximum-considered (XXL1) tsunami scenario at 4 fps, but only if all bridges remain intact after the earthquake. BTW maps for the more likely scenarios where only retrofitted bridges survive (Figure 4-4 and Figure 4-5; Plates 11 and 12) illustrate that seaward of the Necanicum River or on the seaward side of the Highway 101 bridge minimum speeds of > 6 fps are necessary, limiting success to only very fit adults. Evacuation of the elderly at ~2-4 fps (Table 2-2) would be nearly impossible; recall that 17% of Seaside residents in the L1 inundation zone are older than 65 years (Wood and others, 2015). For example, Langlois and others (1997) found that

only 0.5 percent of 72 years old and older pedestrians ≥ 4 fps; 81.1 percent could walk at only 1–3 fps.
in a sample of 989 people could cross an 8-ft course at

Figure 4-1. Evacuation time at 4 fps to reach the eastern bank of the Necanicum River estuary in Seaside with bridges intact. Note that earliest wave arrival at the base of the Necanicum River is on the order of 17–19 minutes after a Cascadia subduction zone earthquake at critical bridges (Plates 7 and 8).

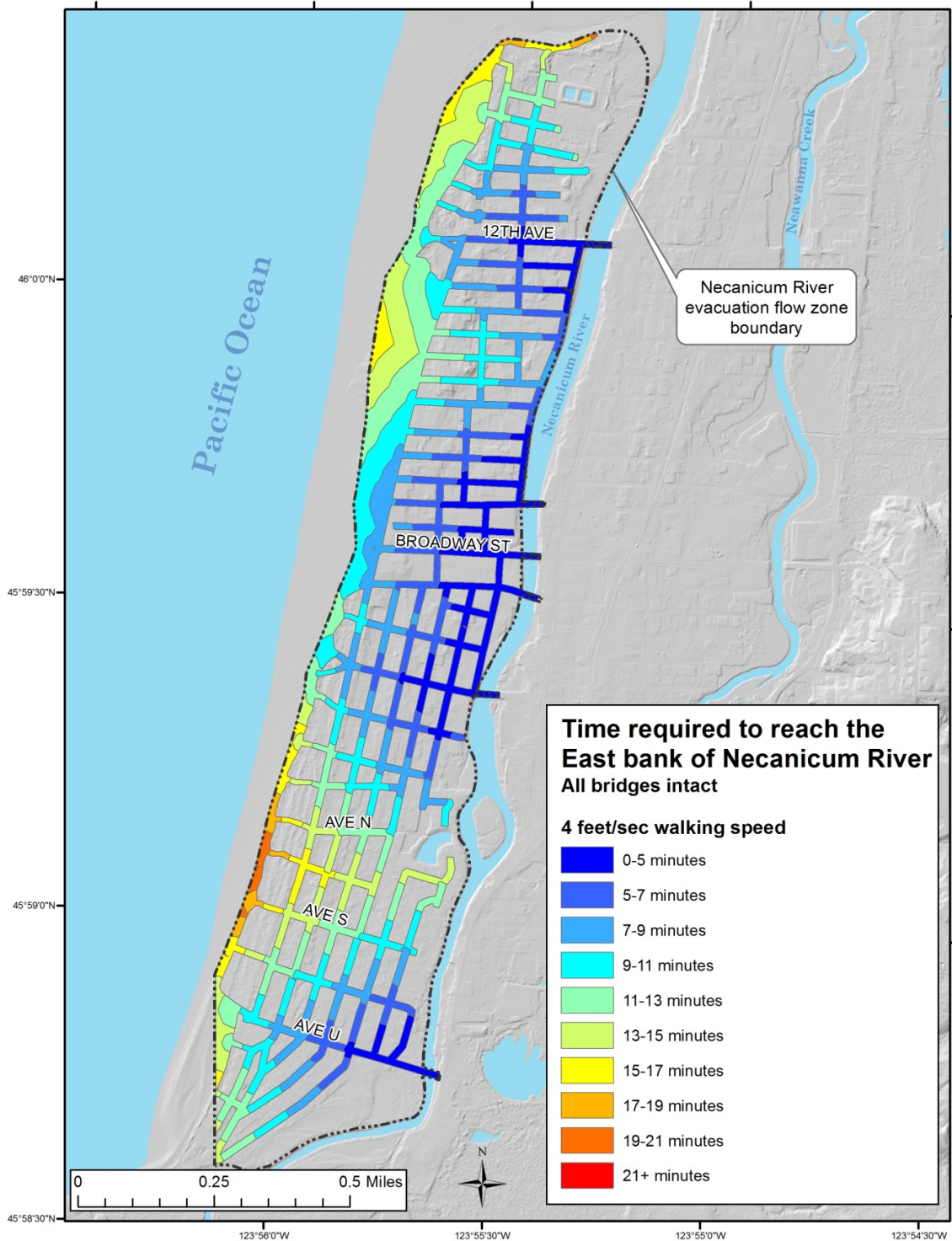


Figure 4-2. Evacuation times at 4 fps to reach the eastern bank of Neawanna Creek in Seaside with bridges intact. Note that earliest wave arrival at Neawanna Creek is on the order of 24–27 minutes after a Cascadia subduction zone earthquake at critical bridges (Plates 7 and 8).

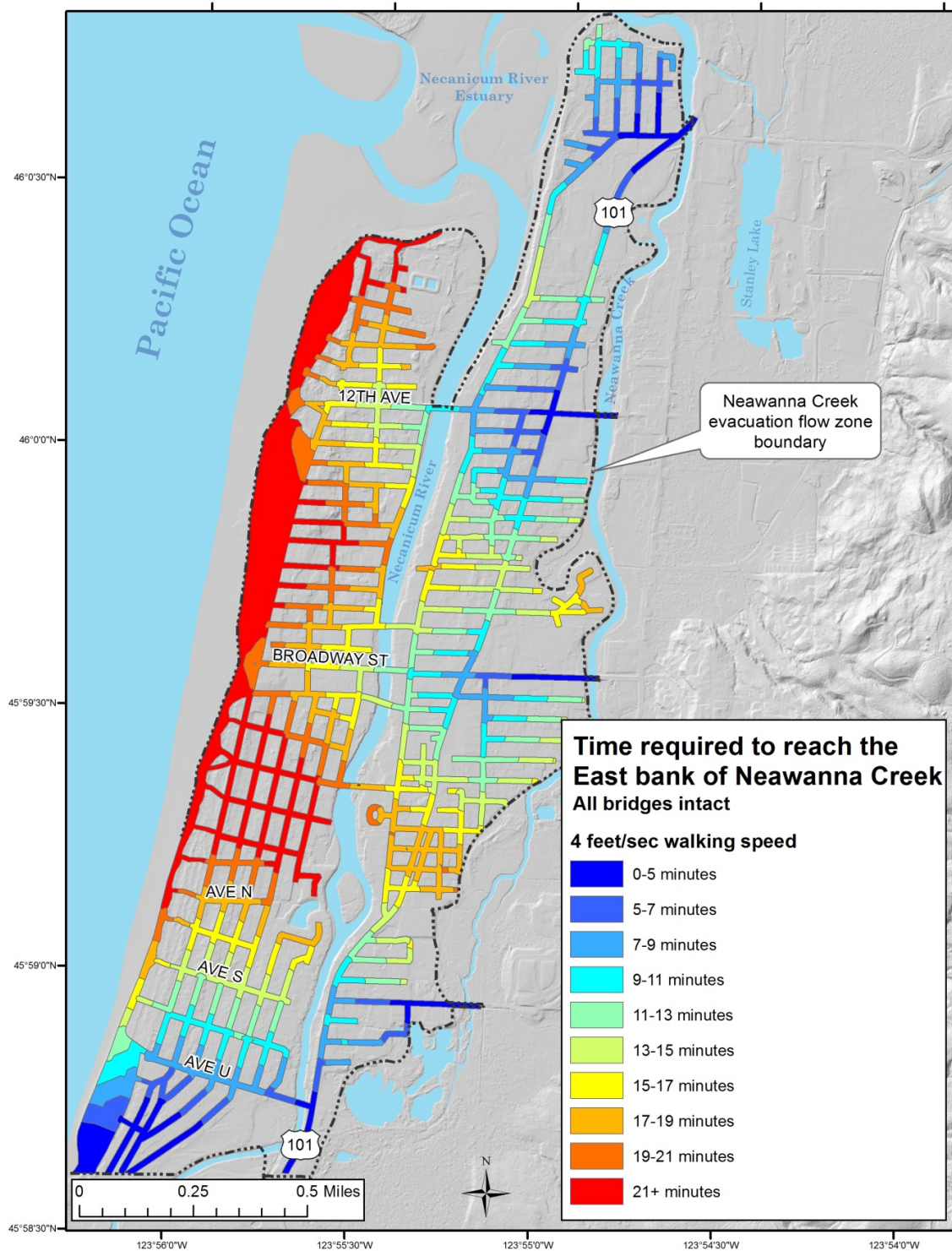


Figure 4-3. Evacuation time at 4 fps to reach the lowest elevation point (earliest tsunami arrival) about 250 feet northeast of the base of Tillamook Head. Note that earliest wave arrival at this point is on the order of 16–18 minutes after a Cascadia subduction zone earthquake (Figure 6).

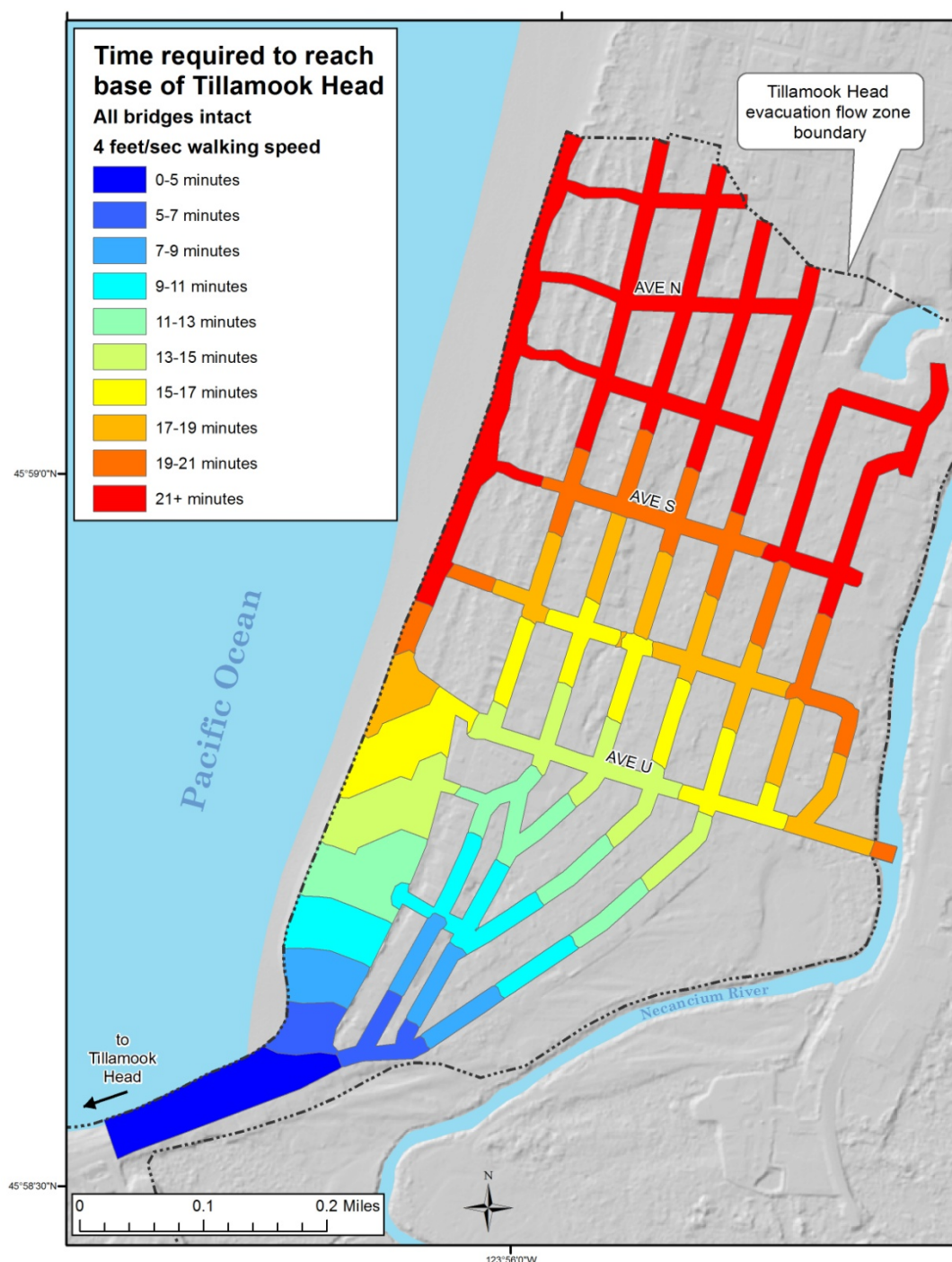


Figure 4-4. Seaside evacuation opportunity map for the XXL1 (maximum-considered event covering ~100% of potential variability) tsunami scenario at 4 fps.

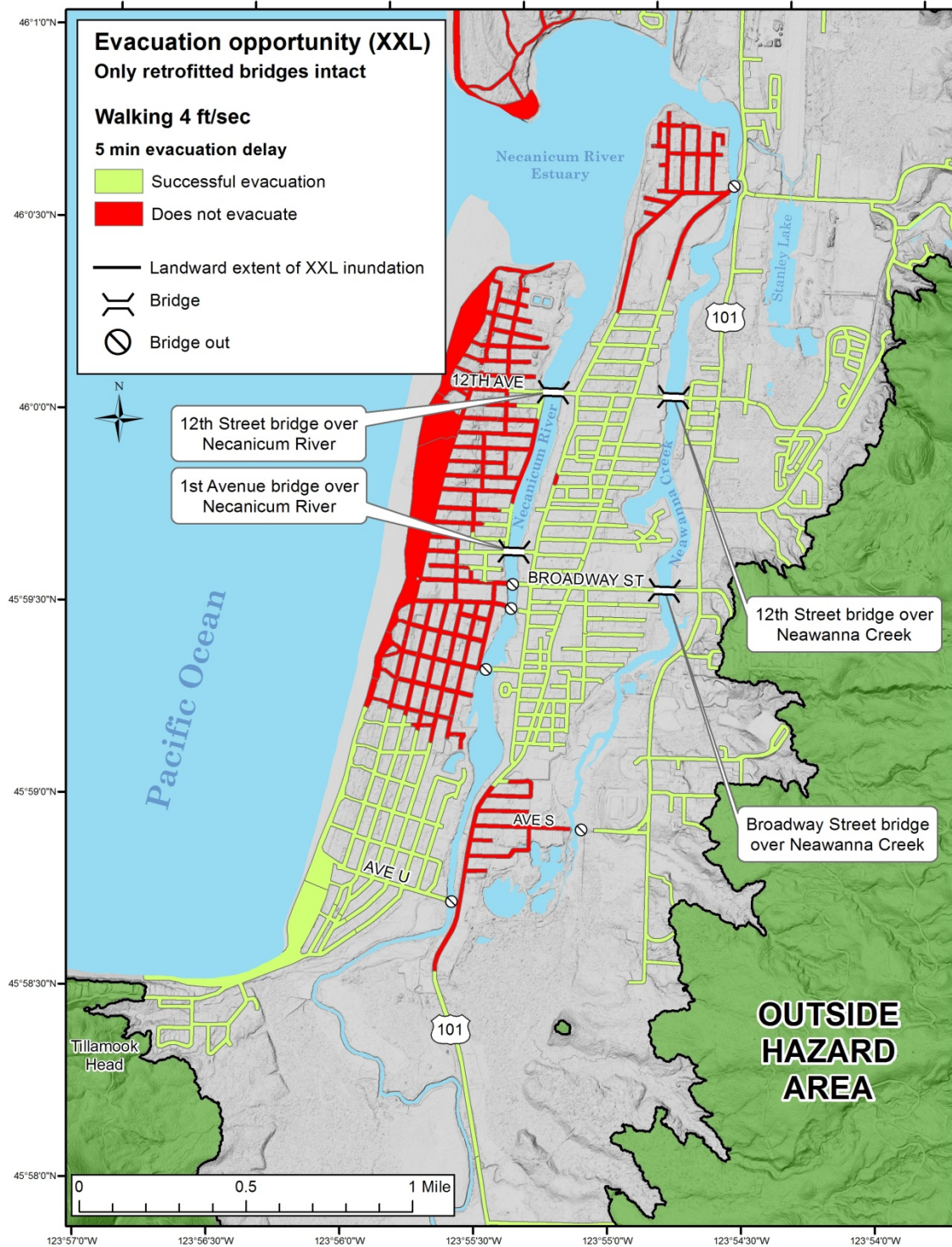


Figure 4-5. Gearhart evacuation opportunity map for the XXL (maximum-considered event covering ~100% of potential variability) tsunami scenario at 4 fps.

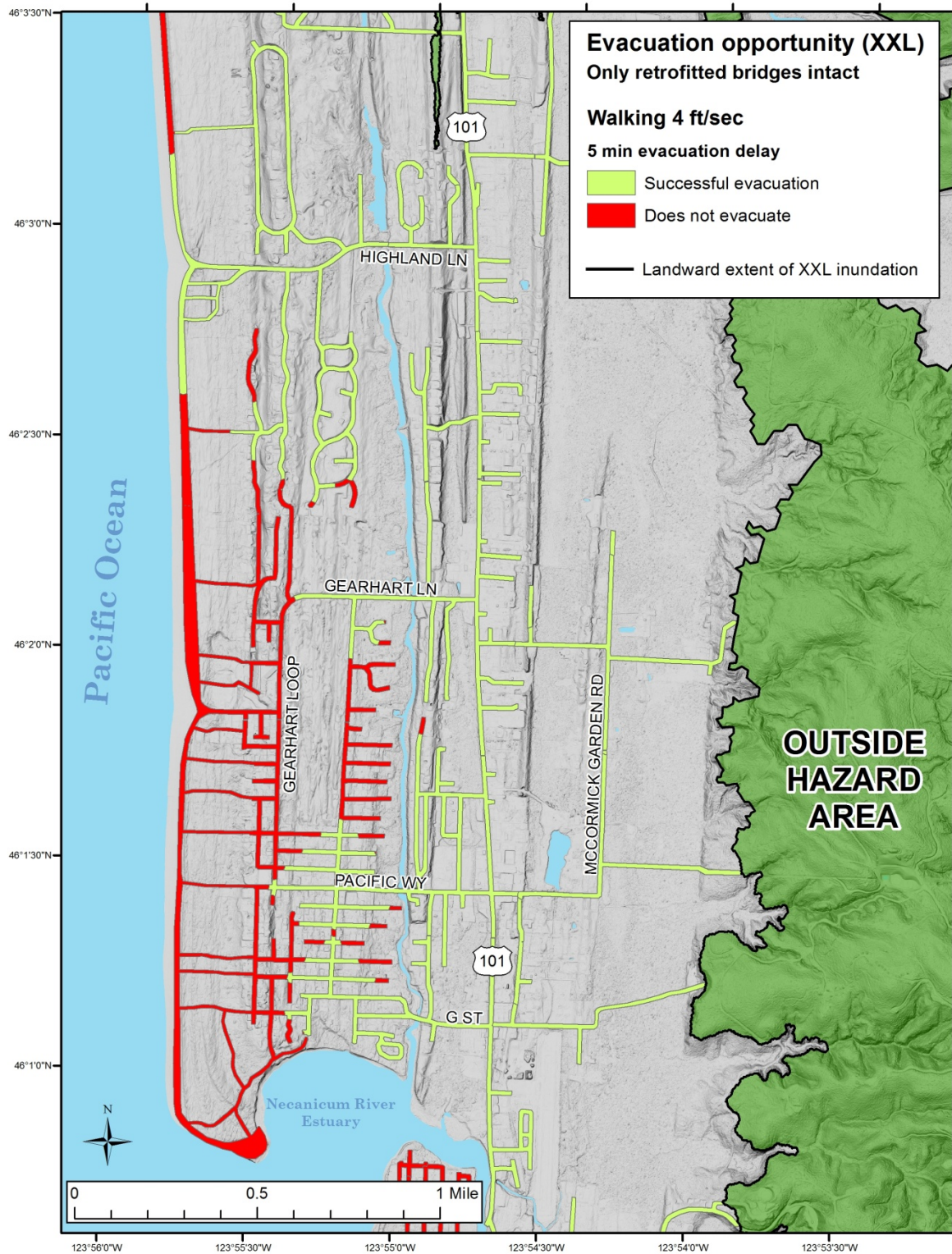
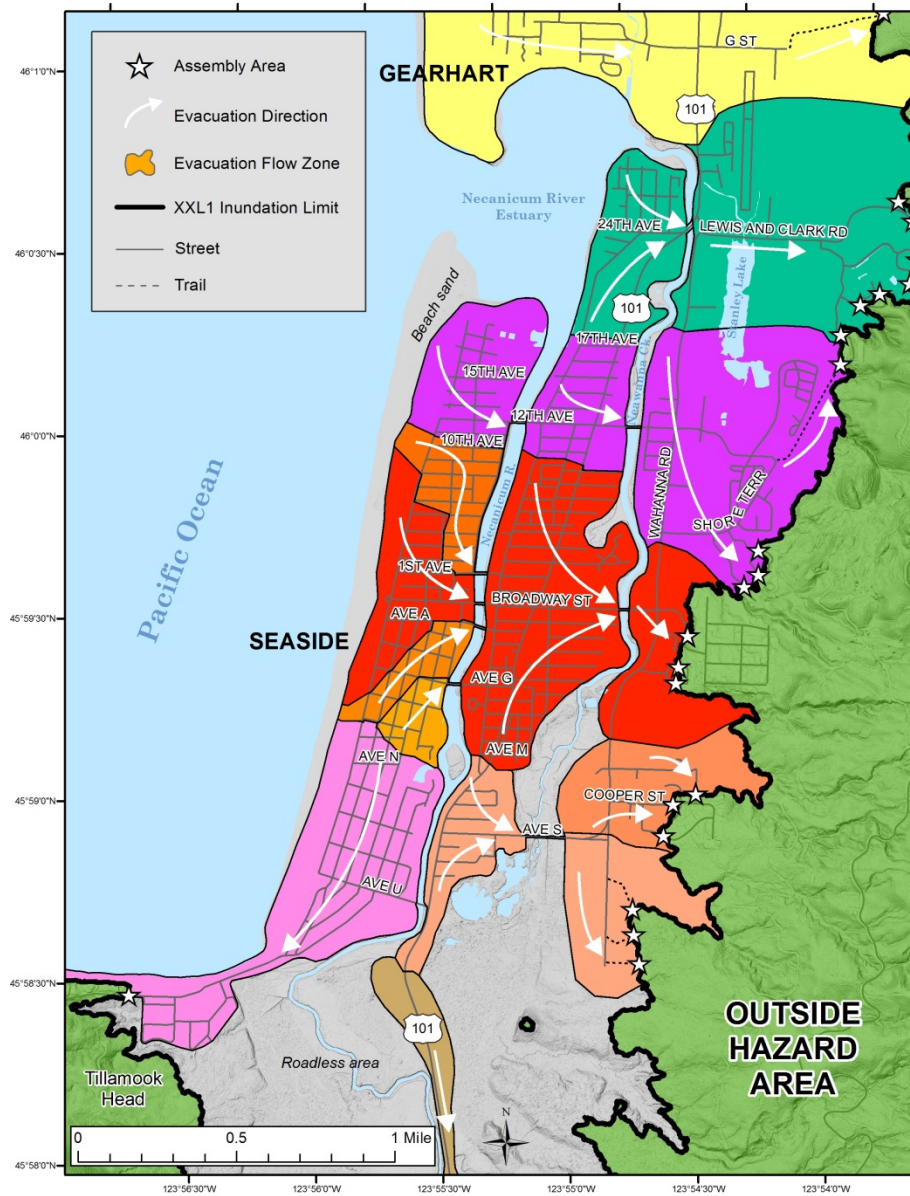


Figure 4-6. Simplified evacuation map showing only evacuation flow zones and direction arrows. In this XXL1 tsunami evacuation scenario, all bridges are assumed to survive the Cascadia earthquake.



Mitigation techniques include installing vertical evacuation structures or providing more lateral evacuation routes. In Seaside the latter would require additional bridges and in Gearhart, improved access to high ground east of the city (Plate 1). However, these two approaches are not equally efficient. For example, construction of more bridges in Seaside would increase evacuation efficiency, but the area positively impacted by each bridge is far smaller than the area

impacted by a local vertical evacuation structure (e.g., compare areas near model vertical evacuation structures in Plates 5 and 6 to areas near bridges in Plate 2). This observation presupposes that any vertical evacuation structures have adequate capacity for the population served and are designed and constructed to remain intact and accessible after the earthquake shaking while also resisting tsunami forces and scour. With regard to structural solutions,

we conclude that increasing the number of retrofitted bridges in Seaside and developing better access to high ground in Gearhart are critical to lateral evacuation, but many areas of westernmost Seaside and Gearhart can be better served by construction of tsunami refuges higher than maximum flow depths for the L1 and XXL1 tsunamis (Figures 13-16). Maximum tsunami flow depth near the Trendwest Resort and Seaside Civic and Convention Center sites is ~50 feet for XXL1 (Figure 5-1; Priest and others, 2013a) and ~30 feet for L1 (Figure 5-2; Priest and others, 2013a). Maximum flow depths in Seaside between the Necanicum River and Neawanna Creek are on the order of ~41–60 feet for XXL1 (Figure 5-1) and 21–30 feet for L1 (Figure 5-2). Maximum flow depths for XXL1 (Figure 5-3) in high parts of Gearhart where L1 does not reach (i.e., dry areas in and around Gearhart Loop Road to 10th Street on Plate 2 and Figure 5-4) are 10–20 feet (Figure 5-3); however, these areas are only ~200–500 feet wide and are located on dunes that could be vulnerable to erosion during a tsunami event. Increasing lateral evacuation at Gearhart is far easier than at Seaside because major bridge construction would be unnecessary and some roads such as Salminen Lane already reach close to high ground (Figure 5-3 and Figure 5-4).

An encouraging finding from this analysis is that evacuation of much of Gearhart at 4 fps should be possible for the L1 scenario, which covers about 95 percent of potential variability in CSZ tsunami inundation. Gearhart is substantially higher in elevation than Seaside so, unlike Seaside, the L1 tsunami scenario leaves a large area dry near the center of the city (Plate 2; Figure 5-4), providing a natural tsunami refuge. However, distal areas such as beaches would still be difficult to evacuate owing to liquefaction, the minimum 5-minute delay caused by earthquake shaking, and the need to travel through significant distances in soft sand.

4.2 Uncertainties and potential improvements

BTW modeling for this study relied on a skilled analyst to examine wave front advance data to determine

where evacuation routes might be compromised by early tsunami arrivals (i.e., establishment of intermediate critical points). An algorithm for placing intermediate critical points would eliminate human error. Likewise, the current BTW method has no algorithm that integrates the tsunami wave front arrival times as a cost in the LCD analysis. For example, the flow zone boundaries are established strictly on the basis of minimum distance to safety without regard to tsunami wave arrivals. If there were a quantitative way to assign costs to wave arrivals along every potential path, both minimum distance and least likelihood of being caught by the tsunami would influence location of flow zone boundaries.

In this approach BTW speeds are limited to paths from the back shore to roads and trails, but starting at points between roads and trails will take longer than from points on roads and trails, so nearest BTW speeds will slightly underestimate or overestimate speed for evacuees starting between roads and trails. In Seaside, distance to a road is generally less than or equal to about half the separation between city streets (approximately 100 ft or 30 m), which creates a 2% error for the western parts of town that are approximately 1 mile (1.6 km) from safety. For evacuees that may have high ground nearby but require travel over natural areas, then BTW speeds may be overestimated by constraining evacuees to roads. These sources of error could be eliminated by running the model for all areas between streets and trails, but this would complicate demarcation of evacuation arrows and pathways by requiring more detailed land cover mapping (e.g., fences) and possibly resulting in pathways that run through private property.

Future BTW mapping could also focus on better defining the evacuation landscape after the initial earthquake. Evacuation speeds could be reduced below model values by ground failures, such as earthquake-induced liquefaction, lateral spreading, and landslides or development of sinkholes from broken water mains. Lowland areas of Seaside are on Holocene sand, silt, and gravel which are variably prone to liquefaction and lateral spreading, while uplands on the east side of town are composed of

Tertiary sedimentary rock prone to landslides (Madin and Wang, 1999). We did not include cost factors for these hazards in the LCD analysis, because of the highly site specific nature of the hazards and high uncertainty of their effect on evacuation speed. Recognition and mitigation of these hazards on key evacuation routes would be a useful means of decreasing this source of uncertainty in the evacuation modeling.

The BTW approach provides minimum speeds to safety for routes defined by the LCD approach, but does not directly evaluate whether those speeds can be maintained along an entire route, for example in sand and up steep hills. As an extreme example, suppose safety is located at the top of a near-shore cliff, the minimum BTW speed would be quite low but the likelihood of getting to safety before wave arrival would be equally low due to the difficulty in scaling the cliff. The practicality of actually covering those distances before the tsunami arrives at safety should still be determined. In this example, one could use the Wood and Schmitdtlein (2012) approach to determine the time it would take a representative adult walking at 4 fps to reach the bottom of the cliff and a separate analysis to the top of the cliff, then compare those times to tsunami arrivals at the bottom and top of the cliff minus any evacuation delay from shaking and behavioral factors. A separate analysis would be required for a mobility-impaired speed. Another approach might be to incorporate into the BTW results safety factors that increase speeds to account for the length of path in difficult terrain. In the example, this would mean that the map would show very high speeds for most of the area seaward of the cliff, indicating that most populations would not be able to evacuate before wave arrival. In a trial, we tried to accomplish this by using the LCD method to artificially increase path distance over difficult terrain, but were not successful in obtaining a mathematically defensible result.

Research devoted to better understanding evacuee behavior is another area for future work. In our case study, five to ten minutes is subtracted from the actual

tsunami wave arrivals to account for delay of evacuation from earthquake shaking and behavioral factors, but this assumption is highly uncertain. The origin time for the tsunami wave arrival time data is the beginning of slip on the CSZ megathrust fault. Once slip begins, there is a variable but potentially significant amount of time required for the natural evacuation signal to arrive in the form of strong shaking. Departure will be additionally delayed by the shaking itself. In the magnitude 9.0 March 11, 2011, Tohoku earthquake, strong shaking lasted about 3–5 minutes (USGS, 2012), and, while coseismic slip on this earthquake was similar to that assumed for the XXL1 scenario (Witter and others, 2011), fault rupture width was larger and length shorter than estimated for a Cascadia event. There are little empirical data on how long it takes people to begin evacuation, but it is reasonable to assume that, as a minimum, walking would be difficult during 3–5 minutes of strong shaking, but there is more uncertainty about the time needed to start evacuation after the shaking. The mean of 7 minutes found in the surveys by the Mas and others (2013) of La Punta, Peru is highly uncertain, as it is not based on data collected immediately following an event. This source of uncertainty could be decreased by systematic collection of behavioral data from modern local tsunami events and promotion of quick, instinctive evacuation through ongoing education programs with a focus on regular community-wide evacuation drills (e.g., Connor, 2005).

BTW analysis is more complex and time consuming than evacuation analyses that determine evacuation times from single speeds (e.g., Wood and Schmitdtlein, 2012). Unlike single speed methods, BTW studies require careful demarcation of intermediate critical points and separate LCD models for every critical point. If rapid analysis of large regions is the objective, single speed methods may be more practical, especially if the primary objective is to compare relative evacuation difficulty among a suite of communities rather than detailed guidance within one community.

5.0 CONCLUSIONS AND RECOMMENDATIONS

The investigation accomplished the primary objective: to provide a quantitative assessment of evacuation difficulty in Seaside and Gearhart. The investigation also developed the BTW (“beat-the-wave”) approach to evacuation analysis that accomplishes in a single map what would require multiple maps in previous approaches such as that of Wood and Schmidtlein (2012); we therefore recommend that BTW maps be the primary products of future detailed analyses of community evacuation. The simpler single-evacuation-speed approach of Wood and Schmidtlein (2012) is more practical for regional analyses.

The results of this study show that evacuation of Gearhart is extremely difficult for a maximum-considered (XXL1) tsunami but reasonably possible for an L1 event covering about 95 percent of possible CSZ events. Evacuation of Seaside west of the

Necanicum River is extremely difficult for either the XXL1 or L1 tsunamis owing to the need to evacuate across a limited number of bridges, only 4 of which have been retrofitted to survive a Cascadia earthquake. Successful evacuation of either Gearhart for XXL1 or westernmost Seaside for XXL1 and L1 will require either evacuation speeds exceeding a moderate walking pace of 4 fps or construction of vertical evacuation facilities. Vertical evacuation options will be particularly critical for successful evacuation of those with limited mobility. Construction of more earthquake resistant bridges across the Necanicum River and Neawanna Creek would also increase evacuation efficiency in Seaside, but the area positively impacted by each bridge is small relative to that of a local vertical evacuation structure. Extension of Salminen Lane to a well-developed assembly area outside of the XXL1 inundation zone would be a cost effective means of greatly increasing efficiency of lateral evacuation of Gearhart.

Figure 5-1. Tsunami maximum flow depth map of Seaside for the maximum-considered XXL1, maximum-considered tsunami scenario. Flow depth data are from Priest and others (2013a); inundation boundary is from Priest and others (2013b).

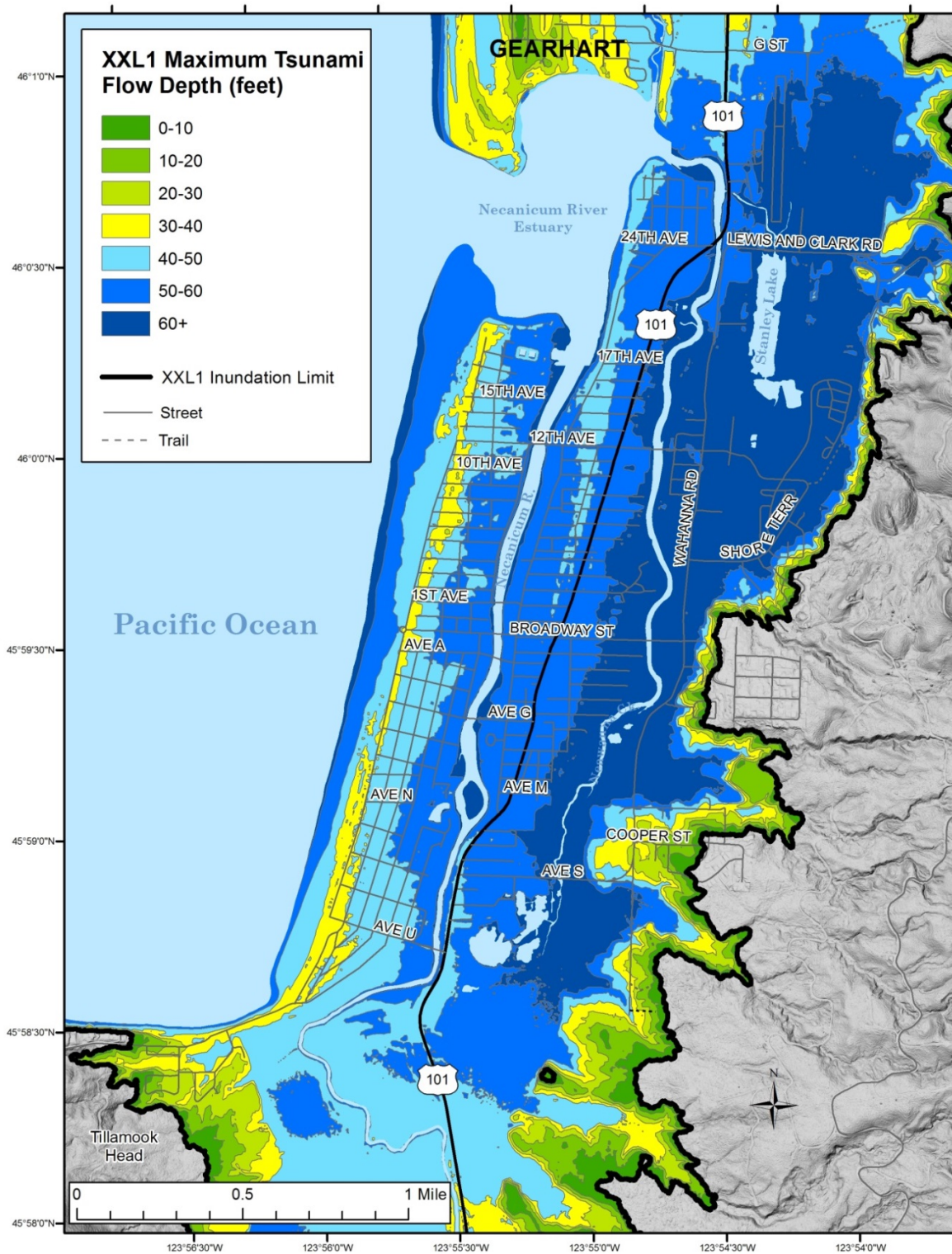


Figure 5-2. Tsunami maximum flow depth map of Seaside for the L1 or “Large” tsunami scenario. Flow depth data are from Priest and others (2013a); inundation boundary is from Priest and others (2013b).

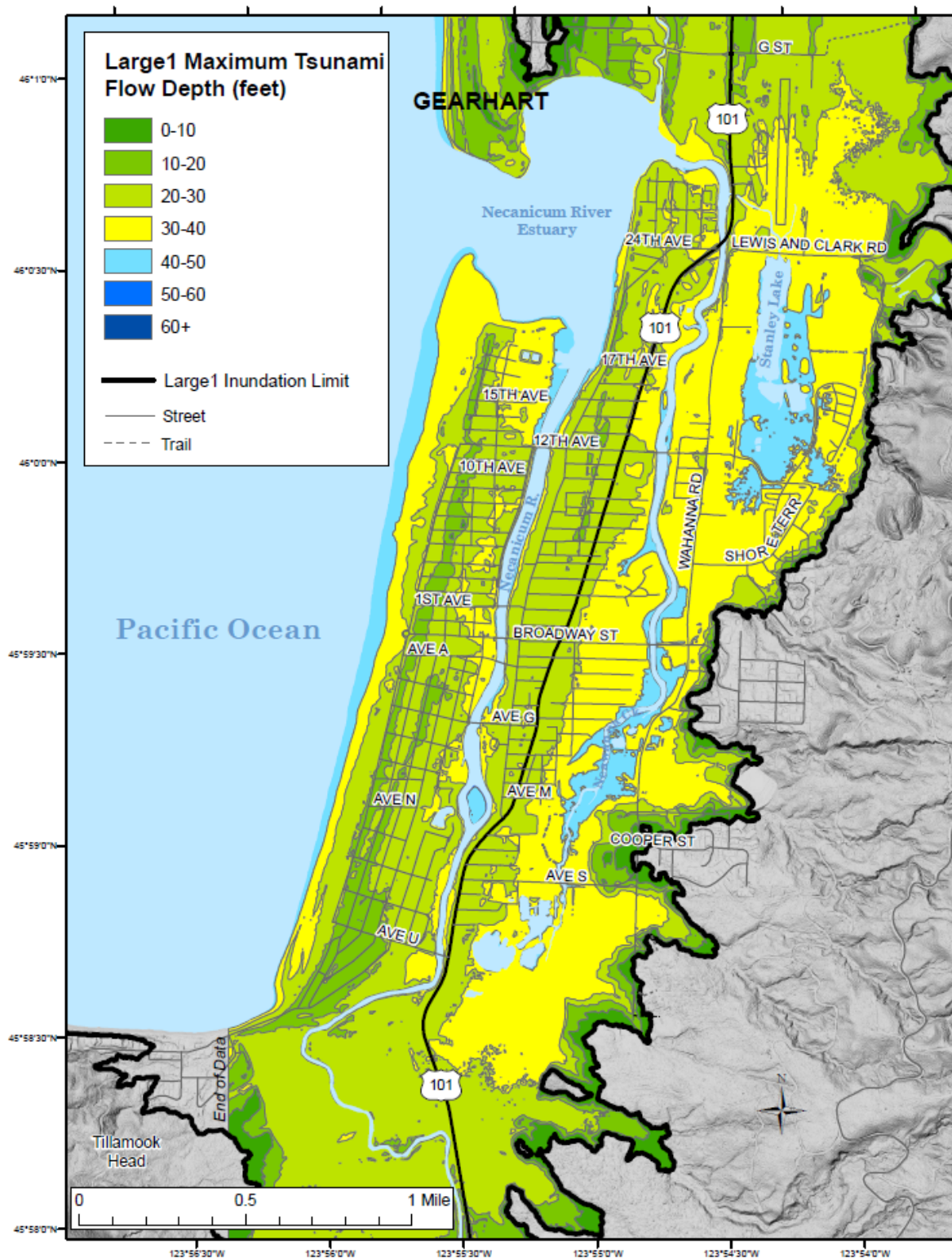


Figure 5-3. Tsunami maximum flow depth map of Gearhart for the maximum-considered XXL1, maximum-considered tsunami scenario. Flow depth data are from Priest and others (2013a); inundation boundary is from Priest and others (2013b).

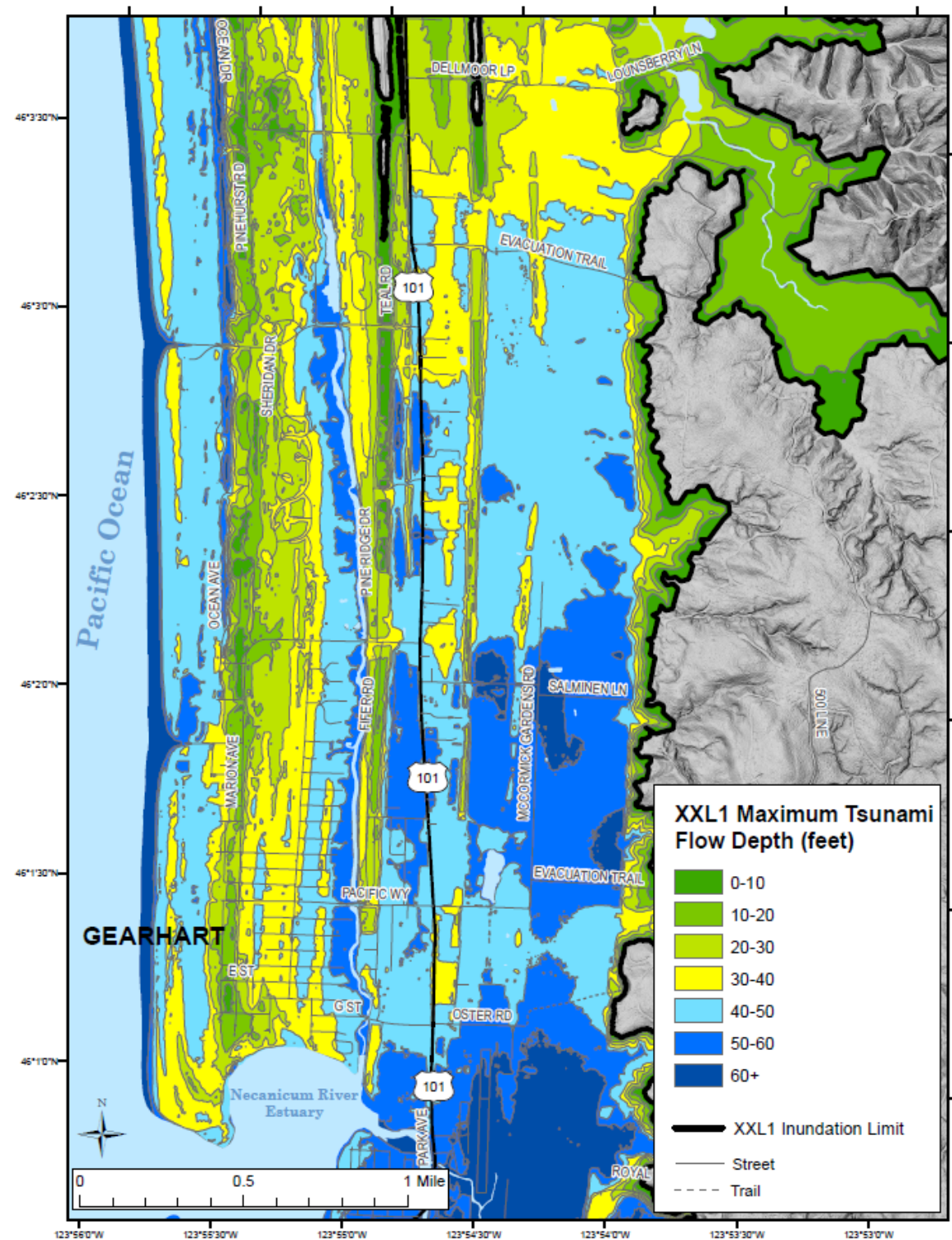
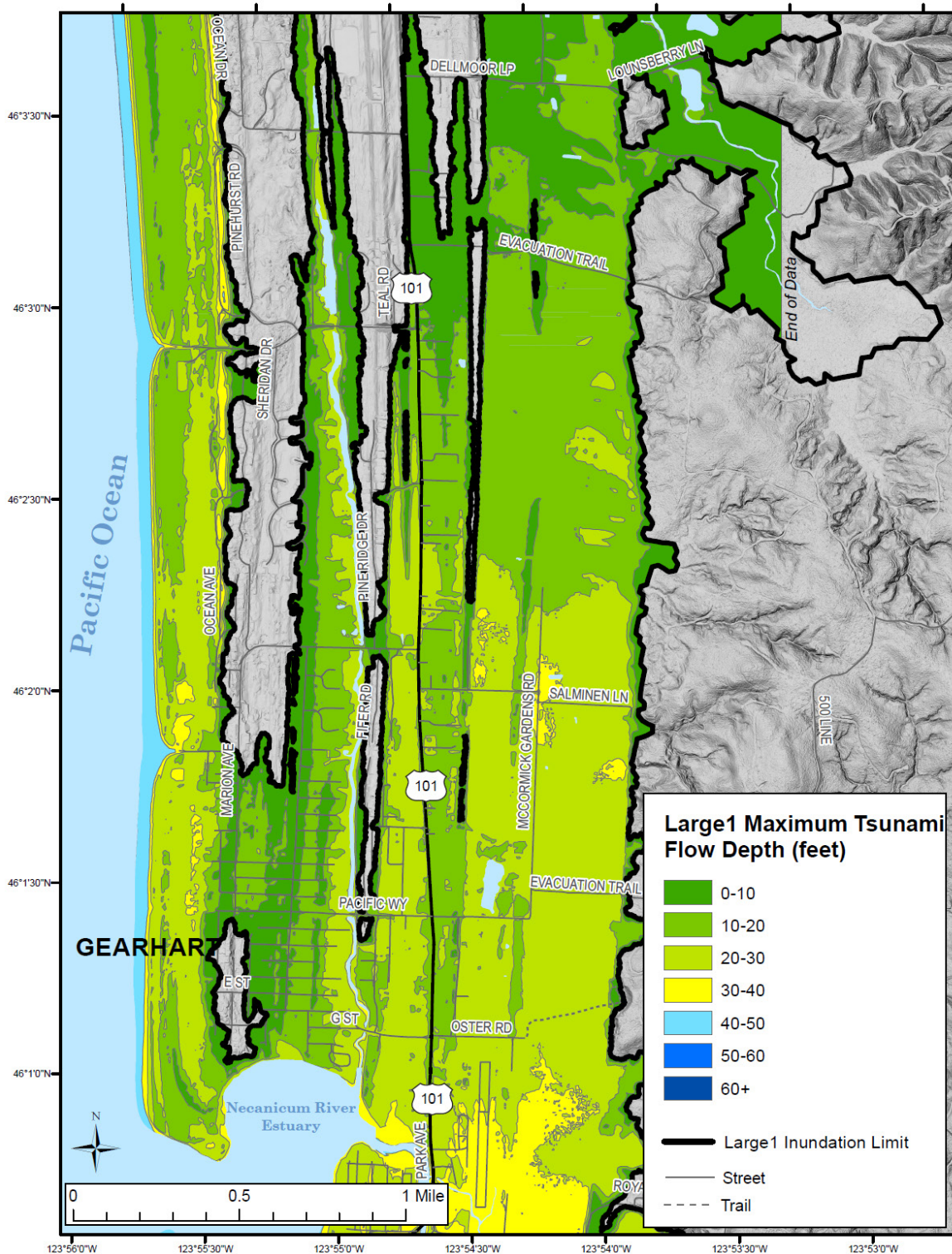


Figure 5-4. Tsunami maximum flow depth map of Gearhart for the L1 or “Large” tsunami scenario. Flow depth data are from Priest and others (2013a); inundation boundary is from Priest and others (2013b).



6.0 ACKNOWLEDGMENTS

This project was funded by the National Oceanic and Atmospheric Administration (NOAA) through the National Tsunami Hazard Mitigation Program under award #NA13NWS4670013. We are grateful for helpful reviews by Nathan J. Wood of the U.S. Geological Survey and Jonathan C. Allan of the Oregon Department of Geology and Mineral Industries.

7.0 REFERENCES

- Connor, D., 2005, The City of Seaside's Tsunami Awareness Program: outreach assessment—how to implement an effective tsunami preparedness outreach program: Oregon Department of Geology and Mineral Industries Open-File Report O-05-10, 86 p. <http://www.oregongeology.org/pubs/ofr/O-05-10.pdf>
- Fraser, S. A., Wood, N. J., Johnston, D. M., Leonard, G. S., Greening, P. D., and Rossetto, T., 2014, Variable population exposure and distributed travel speeds in least-cost tsunami evacuation modelling: *Natural Hazards and Earth System Sciences*, v. 14, no. 11, p. 2975–2991.
- Imhof, E., 1950, *Gelände und Karte: Erlenbach/Zurich*, Eugen Rentsch Verlag, 255 p.
- Langlois, J. A., Keyl, P. M., Guralnik, J. M., Foley, D. J., Marottoli, R. A., and Wallace, R. B., 1997, Characteristics of older pedestrians who have difficulty crossing the street: *American Journal of Public Health* v. 87, no. 3, p. 393–397.
- Madin, I.P., and Wang, Z., 1999, Relative earthquake hazard maps for selected coastal communities in Oregon: Astoria-Warrenton, Brookings, Coquille, Florence-Dunes City, Lincoln City, Newport, Reedsport-Winchester Bay, Seaside-Gearhart-Cannon Beach, Tillamook: Oregon Department of Geology and Mineral Industries, Interpretive Map 10, 25 p., 2 pl., scale 1:24,000. <http://www.oregongeology.org/pubs/ims/IMS-010.zip>
- Margaria, R., 1938, Sulla fisiologia e specialmente sul consume energetico della marcia e della corsa a varie velocita ed inclinazioni del terreno. *Atti Accad Naz Lincei Memorie, in Biomechanics and Energetics of Muscular Exercise* (1976): Oxford, Clarendon Press, p. 299–368.
- Mas, E., Adriano, B., and Koshimura, S., 2013, An integrated simulation of tsunami hazard and human evacuation in La Punta, Peru: *Journal of Disaster Research*, v. 8, no. 2, 285–295.
- Oregon Department of Geology and Mineral Industries, 2013, Tsunami evacuation map for Seaside and Gearhart: Oregon Department of Geology and Mineral Industries. http://www.oregongeology.org/pubs/tsubrochures/SeasideGearhartEvacBrochure-6-3-13_onscreen.pdf
- Paul, S., 2013, What are the right walking and running speeds?: *Runner's World* magazine. <http://www.runnersworld.com/beginners/what-are-right-walking-and-running-speeds> [accessed 4/17/2014]
- Priest, G. R., Goldfinger, C., Wang, K., Witter, R. C., Zhang, Y., and Baptista, A. M., 2009, Tsunami hazard assessment of the northern Oregon coast: a multi-deterministic approach tested at Cannon Beach, Oregon: Oregon Department of Geology and Mineral Industries Special Paper 41, 87 p. plus 7 p. appendix. Includes report, GIS set, time histories, and animations. <http://www.oregon-geology.org/pubs/sp/SP-41.zip>
- Priest, G. R., Witter, R. C., Y. Zhang, Y., Wang, K., Goldfinger, C., Stimely, L. L., English, J. T., Pickner, S. G., Hughes, K. L. B., Wille, T. E., and Smith, R. L., 2013a, Tsunami animations, time histories, and digital point data for flow depth, elevation, and velocity for the Clatsop Project Area, Clatsop County, Oregon: Oregon Department of Geology and Mineral Industries Open-File Report O-13-18. <http://www.oregongeology.org/pubs/ofr/p-O-13-18.htm>

- Priest, G. R., Witter, R. C., Y. Zhang, Y., Wang, K., Goldfinger, C., Stimely, L. L., English, J. T., Pickner, S. G., Hughes, K. L. B., Wille, T. E., and Smith, R. L., 2013b, Tsunami inundation scenarios for Oregon: Oregon Department of Geology and Mineral Industries Open-File Report O-13-19, 14 p. <http://www.oregongeology.org/pubs/ofr/p-O-13-19.htm>
- Priest, G. R., Stimely, L. L., Wood, N. J., Madin, I. P., and Watzig, R. J., 2015, Beat the-wave evacuation mapping for tsunami hazards in Seaside, Oregon, USA: Natural Hazards, p. 1–26. <http://dx.doi.org/10.1007/s11069-015-2011-4>
- Soule, R. G., and Goldman, R. F., 1972, Terrain coefficients for energy cost prediction: Journal of Applied Physiology, v. 32, no. 5, p. 706–708. <http://jap.physiology.org/content/32/5/706>
- Tobler, W., 1993, Three presentations on geographical analysis and modeling; non-isotropic geographic modeling, speculations on the geometry of geography, global spatial analysis: University of Calif., Santa Barbara, National Center for Geographic Information and Analysis Technical Report 93-1, 24 p. http://www.ncgia.ucsb.edu/Publications/Tech_Reports/93/93-1.PDF. Also <http://downloads2.esri.com/campus/uploads/library/pdfs/5864.pdf>
- U.S. Department of Transportation, 2012, Manual on uniform traffic control devices for streets and highways [2009 edition with revisions 1 and 2]: Federal Highway Administration. http://mutcd.fhwa.dot.gov/kno_2009r1r2.htm [accessed 11/25/2014].
- U.S. Geological Survey (USGS), 2012, The March 11 Tohoku earthquake, one year later. What have we learned?: U.S. Geological Survey, Science Features blog post, March 9, 2012. http://www.usgs.gov/-blogs/features/usgs_top_story/the-march-11-tohoku-earthquake-one-year-later-what-have-we-learned/ [accessed 9/9/2014].
- Witter, R. C., Y. Zhang, Wang, K., Priest, G. R., Goldfinger, C., Stimely, L. L., English, J. T., and Ferro, P. A., 2011, Simulating tsunami inundation at Bandon, Coos County, Oregon, using hypothetical Cascadia and Alaska earthquake scenarios: Oregon Department of Geology and Mineral Industries Special Paper 43, 57 p., 3 pl., GIS files, animations. <http://www.oregongeology.org/pubs/sp/p-SP-43.htm>
- Wood, N., and Schmidtlein, M., 2012, Anisotropic path modeling to assess pedestrian-evacuation potential from Cascadia-related tsunamis in the U.S. Pacific Northwest: Natural Hazards, v. 62, no. 2, p. 275–300. <http://link.springer.com/content/pdf/10.1007%2Fs11069-011-9994-2.pdf>
- Wood, N., Jones, J., Spielman, S., and Schmidtlein, M., 2015, Community clusters of tsunami vulnerability in the US Pacific Northwest: Proceedings of the National Academy of Sciences, v. 112, no. 17, 5343–5359. doi: 10.1073/pnas.1420309112. <http://www.pnas.org/content/112/17/5354.full.pdf>
- Yeh, H., Fiez, T., and Karon, J., 2009, A comprehensive tsunami simulator for Long Beach Peninsula. Phase 1: framework development: Tacoma, Wash., Washington State Military Department, 27 p.